ELECTROCHEMICALLY SWITHABLE PLASMONIC SURFACES

A THESIS
SUBMITTED TO THE MATERIALS SCIENCE AND
NANOTECHNOLOGY PROGRAM
OF THE GRADUATE SCHOOL OF ENGINEERING AND SCIENCE
OF BILKENT UNIVERSITY
IN PARTIAL FULLFILMENT OF THE REQUIREMENTS
FOR THE DEGREE OF
MASTER OF SCIENCE

By
Nihat Serkan KARAYALÇIN
January , 2014

I certify that I have read this thesis and that in my opinion it is fully adequate, in scope and in quality, as a thesis for the degree of Master of Science.

_____

Asst. Prof. Dr. Aykutlu Dana (supervisor)

I certify that I have read this thesis and that in my opinion it is fully adequate, in scope and in quality, as a thesis for the degree of Master of Science.

_____

Assoc. Prof. Dr. Cengiz Koçum

I certify that I have read this thesis and that in my opinion it is fully adequate, in scope and in quality, as a thesis for the degree of Master of Science.

_____

Assist. Prof. Dr. Bülend Ortaç

Approved for the Graduate School of Engineering and Science:

_____

Prof. Dr. Levent Onural

Director of the Graduate School

ABSTRACT

ELECTROCHEMICALLY SWITHABLE PLASMONIC SURFACES

Nihat Serkan KARAYALÇIN
M.S. in Materials Science and Nanotechnology
Supervisor: Assist. Prof. Dr. Aykutlu Dana
January 2014

In this study, we design and produce grating coupled surface plasmon surfaces which are switched by electrochemistry. Grating structures are fabricated using digital versatile discs (DVDs) which are commercially available. According to atomic force microscopy (AFM) results, we categorize the different grating structures in two groups, namely shallow and deep gratings. Plasmonic properties of the surfaces are investigated using numerical simulations. Gold and silver are used as plasmon supporting metallic layers on gratings. Refractive index sensitivity of the plasmon resonances are studied using deionized water, air and glycerol solutions as the dielectric media and results are compared with simulations. Experimental results are coherent with the simulations in terms of reflection spectra.

Electrochemical switching of plasmonic properties may have applications in tunable and switchable filters, as well as enhanced colorimetric sensing. We deposit ultrathin films of copper on plasmonic surfaces and investigate reversible changes in the plasmonic properties. Copper sulfate is selected as the electrolyte. Cyclic voltammetry is performed on plasmonic surfaces while monitoring optical reflectance. Copper is observed to deposit in the form of nanoislands on silver and gold films rather than uniform thin films. The effect of copper deposition on the plasmonic properties of the grating structure is simulated by Lumerical software and

is seen to be two fold. For small effective thickness of copper nanoislands, the plasmon resonance condition shifts, whereas for thicker copper deposition plasmonic resonances are eliminated.

Finally, copper's oxidation and reduction reactions are controlled by changing applied voltage thus shifting the resonance wavelength. Resonances are switched reversibly multiple times not only for different molarities but also for different grating sructures and plasmon supporting metallic layers . In summary, we demonstrate that plasmonic properties of nanostructured metallic surfaces can be controlled by electrochemistry. Switchable resonance surfaces can be used as dynamic filters or may enhanced contrast in plasmon resonance imaging applications.

Keywords: Plasmonics, Grating Coupled Surface Plasmon Resonance, Electrochemistry, Dynamic filters, Surface Plasmon Resonance Imaging

ÖZET

ELEKTROKİMYASAL OLARAK DEĞİŞTİRİLEBİLEN PLAZMONİK YÜZEYLER

Nihat Serkan KARAYALÇIN
Yüksek Lisans, Malzeme Bilimi ve Nanoteknoloji Bölümü
Tez Yöneticisi: Yrd. Doç. Dr. Aykutlu Dana
Ocak 2014

Bu çalışmada , elektrokimyasal olarak değiştirilebilen kırınım ağı kuplajlı yüzey plazmon yüzeylerinin tasarımı ve üretimini gerçekleştirdik. kırınım ağı yapılarını , ticari olarak temin edilebilen çok amaçlı sayısal diskler(DVDs) kullanılarak ürettik. Atomik kuvvet mikroskobu sonuçlarına göre, kırınım ağı yapılarını sığ ve derin olarak 2 kategoriye ayırdık. Numerik simülasyonlar kullanılarak yüzeylerin plazmonik özellikleri inceledik. Altın ve gümüşü, kırınım ağı yapıları üzerinde plazmon destekleyici metalik katman olarak kullandık. Plazmon rezonanslarının kırılma indisi hassasiyetini , deiyonize su ,hava ve gliserol solüsyonunu dielektrik ortam olarak kullanarak araştırdık. Deneysel sonuçların yansıma spektumu cinsinden numerik simülasyonlarla uyumlu olduğunu gözlemledik.

Plazmonik özelliklerin elektrokimyasal olarak değiştirilebilirliği, ayarlanabilir ve değiştirilebilir filtreler ayrıca artırılmış kolorimetrik algılama uygulamalarında kullanılabilir. Plazmonik yüzeylerin üzerine çok ince bakır tabaka indirgedik ve plazmonik özelliklerde geri çevrilebilir değişiklikleri araştırdık. Elektrolit olarak bakır sülfat seçtik. Plazmonik yüzeylere periyodik voltmetri uygularken optik yansımayı takip ettik. Bakırın, altın ve gümüş filmlere düzgün ince tabakalar yerine nanoadalar şeklinde indirgendiğini gözledik. Bakır indirgenmesinin kırınım ağı yapılarının plazmonik özellikleri üzerindeki etkileri Lumerical yazılımını kullanarak

simüle ettik ve etkinin 2 katı olduğunu gözledik. Bakır nanoadaların küçük efektif kalınlığı için plazmon rezonans durumunun kaydığı , kalın bakır indirgenmesinde plazmonik rezonansın yok olduğunu gözlemledik.

Sonunda, bakır yükseltgenme ve indirgenme reaksiyonlarını uygulanan voltaj değiştirilerek kontrol ettik ve bu sayede rezonans noktasını kaydırdık. Rezonansları sadece değişik molarite için değil ayrıca değişik kırınım ağı yapıları ve değişik plazmon destekleyici metalik katmanlar içinde birçok kez geri çevrilebilir şekilde değiştirdik. Özetlemek gerekirse , nanoyapılı metalik yüzeylerin plazmonik özelliklerinin elektrokimya yardımıyla kontrol edilebileceğini kanıtladık. Değiştirilebilir rezonans yüzeyler, dinamik filtreler yada plazmon rezonans görüntülemede kontrast artırma uygulamalarında kullanılabilir.

Anahtar Kelimeler: Plazmonik , Kırınım Ağı Kuplajlı Yüzey Plazmon Rezonans, Elektrokimya , Dinamik Filtre, Yüzey Plazmon Rezonans Görüntüleme

Acknowledgement

I would like to thanks to my supervisor Dr. Aykutlu Dana for his valuable guidance.

I would also like to thank my group members; Sencer Ayaş, Öner Ekiz, Hasan Güner, Burak Türker and Mustafa Ürel.

I owe thanks to my parents and friends for their support and patience.

Finally I acknowledge UNAM for the financial support.

Dedicated to my family

Table of Contest

1.Introduction 1

2.Theoretical Background 5

2.1 Surface Plasmon 5

2.1.2 Excitation Methods of Surface Plasmons 9

2.1.2.1 Prism Coupling 10

2.1.2.2 Grating Coupling 11

2.2 Electrochemistry 12

3. Characterization of Grating Structures 15

3.1 Surface Topography of Grating Structures 15

3.2 Numerical Simulations 18

4.Production 24

4.1 Plasmonic Gratings 24

4.2 Electrochemical Cell 26

4.3 Experimental Setup 29

4.4 Electrolites 29

5. SPR and Electrochemical Experiments, Lumerical Simulations 30

5.1. SPR Experiments 30

5.2 Cyclic Voltagram 36

5.3 Lumerical Simulations 39

6. Electrochemically Switchable Plasmonic Surfaces 42

6.1 Shallow Grating Experiments..... 42

6.2 Deep Grating Experiments 45

7. SPR Colorimetric Sensing and Imaging **48**

7.1 SPR Colorimetric Imaging 48

7.2 SPR Colorimetric Sensing..... 50

8.Conclusion and Future Work **52**

List of Figures

Figure 2.1 : Surface plasmons between metal ,dielectric media 5
Figure 2.2 : Geometry for wave propagation at metal-dielectric interface 6
Figure 2.3 : Dispersion relations between wavevector of light in air and wavevector of plasmon 9
Figure 2.4: Prism coupling geometry : (a) Kretschmann configuration , (b) Otto configuration 10
Figure 2.5: The plasmonic dispersion relation for grating coupling 12
Figure 2.6: Electrochemical reaction process 13
Figure 3.1: AFM image of Verbatim Blueray Disc ; (a) 3d surface topography, (b) Period and depth 16
Figure 3.2: AFM image of Maxell Pro-x DVD ; (a) 3d surface topography, (b) Period and depth 17
Figure 3.3: AFM image of Maxell R+DVD; (a) 3d surface topography, (b) Period and depth 17
Figure 3.4: (a)Numeric aperture of experimental setup , (b) Diffraction Angle v.s Wavelength of Reflected Orders 18
Figure 3.5: Wavelength interrogation simulation of blueray grating structure when DI water as dielectric media and Al, Au, Ag as plasmon supporting metallic layer 19
Figure 3.6: Wavelength interrogation simulation of Shallow grating structure when DI water as dielectric media and Al,Au,g as plasmon supporting metallic layer 20
Figure 3.7: Wavelength interrogation simulation of Deep grating structure when DI water as dielectric media and Al, Au, Ag as plasmon supporting metallic layer 20
Figure 3.8: Wavelength interrogation simulation for different thicknesses of copper layer on Ag deposited surface when DI water as dielectric media 21
Figure 3.9: Wavelength interrogation simulation for different thicknesses of copper layer on Ag deposited surface when DI water as dielectric media 22

Figure 3.10: Angle interrogation simulation of Deep grating structure with different incident ligth angle; DI water as dielectric media and Au as plasmon supporting metalic layer 22
Figure 4.1 :Sample preparation steps : (a)splitting it into 2 parts, (b) nitric acid threatment 24
Figure 4.2: (a) AFM image of gratings after metal deposition (b) Sem image of coated sample 25
Figure 4.3: Xps image of sample : survey analysis 26
Figure 4.4: First version of electrochemical cell 27
Figure 4.5: Final version of channel 28
Figure 4.6: Optical experimental setup 29
Figure 5.1: Reflection spectrum of Shallow grating structure when 60 nm Ag on 10 nm germanium as metallic layer, DI water as dielectric media 31
Figure 5.2: Reflection spectrum of Shallow grating structures when 60 nm Ag on 10 nm Ge as metallic layer, air as dielectric media 31
Figure 5.3: Reflection spectrum of Shallow grating structures when 60 nm Au on 10 nm Ge as metallic layer, air as dielectric media 32
Figure 5.4: Reflection spectrum of Shallow grating structure(other side of DVD's) when 60 nm silver over 10 nm germanium as metallic layer, air as dielectric media 32
Figure 5.5: Reflection spectrum of Shallow grating structure(other side of DVD's) when 60 nm Ag over 10 nm Ge as metallic layer, DI water as dielectric media. 33
Figure 5.6: Reflection spectrum of Deep grating structure when %100 DI water(n=1.33) as dielectric media 34
Figure 5.7: Reflection spectrum of Deep grating structure when %36 glycerol solution (n =1.3787) as dielectric media 34
Figure 5.8: Reflection spectrum of Deep grating structure when %53 glycerol solution (n=1.4025) as dielectric media 35
Figure 5.9: Reflection spectrum of Deep grating structure when %100 glycerol (n=1.47399) as dielectric media 35
Figure 5.10: Cyclic voltagram of 0,05 M CuSO4 solution between ±0,4 V 36
Figure 5.11: XPS result after cyclic voltagram 37

Figure 5.12: Sem image of silver coated grating surface with 0.05M CuSO4 solution after applying -0,4 volt during ; (a)3 seconds , (b)7 seconds, (c)10 seconds, (d)15 seconds 38
Figure 5.13: Grating structure simulated by Lumerical software 39
Figure 5.14: Simulation for 90 nm width periodically empty area with 10,40,60 nm heights copper nanoislands..... 40
Figure 5.15: Simulation for 80 nm width periodically empty area with 10,40,60 nm heights copper nanoislands..... 40
Figure 6.1: ±0,4 V applied voltage; silver as plasmon supporting metallic layer and 0,01 M CuSO4 solution as dielectric media..... 43
Figure 6.2: ±0,4 V applied voltage; silver as plasmon supporting metallic layer and 0,05 M CuSO4 solution as dielectric media..... 43
Figure 6.3: ±0,4 V applied voltage; silver as plasmon supporting metallic layer and 0,1 M CuSO4 solution as dielectric media..... 44
Figure 6.4: ±0,4 V applied voltage; silver as plasmon supporting metallic layer and 0,02 M CuSO4 solution as dielectric media..... 45
Figure 6.5: ±0,4 V applied voltage; silver as plasmon supporting metallic layer and 0,05 M CuSO4 solution as dielectric media..... 45
Figure 6.6: ±2V applied voltage; gold as plasmon supporting metallic layer and 0,05 M CuSO4 solution as dielectric media..... 46
Figure 6.7: Sem image of silver coated grating structure after switched several times 47
Figure 7.1: Rectangular structures on Deep grating based golden surface 49
Figure 7.2: Surface image of Deep grating based golden surface with 0,02M CuSO4 49
Figure 7.3: Images of surfaces according to applied voltage and period..... 51
Figure 8.1: (a) top view, (b) bottom view of potantiostat circuit..... 53

CHAPTER 1

Introduction

The excitation of surface plasmons is first observed from unusual reflected pattern when polarized light is sent on metallic surface. Later, scientists started to use surface plasmons for practical applications such as characterization of thin films. Gas sensing application is the first attempt to use Surface Plasmon Resonance (SPR) as sensor [1]. After that, the number of studies based on SPR biosensor application continiously increased. In the later 1980s, SPR is used first time for imaging by Rothenhausler and Knoll [2]. Because SPR provides label-free and real time measurments, interest in SPR studies increased over the last decades. SPR is one of the most widely used method for implementing label free biosensors [3-10]

Connection between electric and chemistry is set by discovery of Alessandro Volta in 1973 .Volta produced the primitive battery by putting different metal at opposite side of moistened paper. In 1800, Nicholson and Carlisle seperated water into hydrogen and oxigen by applying voltage (electrolysis). After that, Faraday indicated the relation between applied current and amount of electrolysis production. Even though electrochemistry is discovered in 1800s , its applications accelerated after 1950s. Like SPR , electrochemistry is used in sensor applications [11-19]

There is a large number of publications on using electrochemistry and plasmon resonances for biosensor applications. Li et al. use SPR and electrochemical measurements together to investigate interaction between α-actinin and negatively charged lipids membrane. They demonstrate that α-actinin can bind to negatively charged lipids membrane by change in SPR and cyclic voltagram results. They use the both techniques to increase the reliability [20]. Toda et al. use SPR to produce

electrocemical enzyme immunoassay. They immobilize antibody on gold electrode by monitoring the SPR signal [21].

Some researchers realize the high potential of combining electrochemistry and SPR. Panta et al. observe the deposition and stripping steps of mercury due to cyclic voltagram by SPR [22]. Also Huang et al. detect intermediate reaction product by SPR. They control hydroquinone–benzoquinone (HQ–BQ) reaction by cyclic voltagram and semiquinone radical anion (BQ) is detected as intermediate reaction product[23]. On the other hand Vasjari et al. use SPR to observe the redox reactions of mercury. They use cyclic voltagram to control oxidation and reduction reactions of mercury and measure the changes in SPR angle.[24]

Plasmonic imaging by electrochemistry studies also find place in more prestigious journals. Tsuboi et al. use electrochemical deposition of silver nano particles on Indium Tin Oxide (ITO) to make multicolor devices by using localized plasmon resonance (LSPR) properties of silver nanoparticles. They are able to tune the plasmonic properties across the visible spectrum in this way.[25] Shan et al. enhance contrast in plasmonic imaging to determine electrochemical current due to redox reactions of $Ru(NH_3)^{3+}$ on gold electrode.[26]

Especially inspired from Shan et al. study, possibility of monitoring thin layers by electrochemically control of surface's plasmonic properties with grating coupled mechanism is our main motivation. For these purpose, we design and produce plasmonic surfaces based on gratings which fullfits all the requirements of the excitation of plasmons with in a compact and economical setup. We realize dynamic filters and plasmonic imaging with these structures. Accoding to results presented in this thesis, we may assert that deep grating based plasmonic surfaces have great potential in colorimetric biosensor applications.

We organized the thesis as follows ;

In chapter 2, we explain the surface plasmon, and the dispersion relation of surface plasmons by deriving the equations. We mention the most commonly used methods for excitation of surface plasmons; grating and prism coupling. We explain the Kretschmann and Otto configuration for prism coupling method in detail. We give the details of the grating coupling mechanism while indicating benefits. Finally we explain why we use grating coupling method in this study.

In chapter 3, we characterize the commercially available Digital versatile discs (DVDs). DVDs are used as the plasmonic platform because of their commercially availability and presence of perfect fabricated structures. We determine the surface topography of DVDs by Atomic Force Microscopy(AFM). According to AFM results, we categorize the gratings in two groups proportional to their depths; namely Deep and Shallow. We investigate the plasmonic properties of the gratings against different plasmon supporting layers and dielectric medias by numerical simulations. We identify that surface plasmon resonance based on Shallow grating is usually sharp , while Deep grating based plasmon resonance is usually broad. Besides we simulate copper nanolayer on the surfaces for both gratings and observe shifts in resonance upon electrochemical modification thus we demonstrate that swithable plasmonic surfaces can be realized by electrochemical control of redox reactions. Finally we simulate angle dependance of the gratings and determine that smooth results can be achived with 0^o incident light angle.

In chapter 4, we give details of obtaining the plasmonic gratings from commercial DVDs. First we obtain the burried grating structure by splitting the DVDs and clean before metal deposition by nitric acid and ultrasonic cleaner. Then we deposit gold and silver as plasmon supporting layer and germanium as adhesive layer by thermal evaporator to produce plasmonic surfaces. We design and produce electrochemical cell multiple times to eliminate bubble and conduction problem. We describe the optical experimental setup for 0^o incident angle measurements. We explain the configuration of the optical experimental setup in detail .

In chapter 5 , we perform SPR experiments to observe coherence between the samples and numerical simulation results for both grating structures. According to experimental results, we determine the samples are produced appropriately. At the same time , we calculate sensitivities of the systems and compare them with literature. We perform cyclic voltagram experiments to investigate electrochemical properties of copper sulfate solutions. We determine redox currents for solutions with different concentrations thus we observe that $\pm$ 0.4 volt guarantees the oxidation and reduction for all solutions. Based on this result, we decide to perform constant voltage experiments rather than cyclic voltagram. We apply constant

voltage with different period to different samples to investigate copper deposition formation on surface by Scanning Elecron Microscopy(SEM). According to the SEM images, we determine that copper deposites on surface as nanoislands rather than thin layers. We simulate effect of copper nanoislands on plasmonic properties of the surfaces by Lumerical software. We determine that for different thicknesses and densities of copper nanoislands, plasmon resonance shifts.By this way, we demonstrate theoretically that plasmonic properties of the surfaces can be controlled by electrochemistry

In chapter 6, we start electrochemical SPR experiments. According to the experiments, we show that plasmonic properties of surfaces can be controlled by electrochemistry. We perform experiments not only for different grating structures but also for different plasmon supporting metallic layers. As a result of the experiments, we notice that origin of resonance shifts in course of time after switching multiple times when silver as plasmon supporting metallic layer. We repeat the experiments for gold as metallic layer with higher applied voltage and observe no such problems for these conditions. We take image of surface by SEM after the experiments and determine the source of the problem that copper existence on surface after oxidation process.

In chapter 7, we use Deep grating based plasmonic surfaces's broad resonance profile for plasmonic imaging. For this purpose, we produce rectangular structures on surfaces by optical litography and etching process. We image these structures on golden surfaces by simple camera. On the other hand, we perform the electrochemical experiments and provide color changes of surface reversibly. By this way , we demonstrate that the Deep grating based plasmonic surfaces can be used for colorimetric biosensor applications.

In last chapter , we conclude the study and explain the future works in detail. In order to control electrochemical reactions precisely, we decide to change the system with 2 electrodes to 3 electrodes is called potentiostat circuit. We explain the potentiostat circuit which is produced in detail. Finally, we mention about the future plan that designing a smart phone attachment to demonstrate plasmonic imaging can be performed by smart phones,

CHAPTER 2

Theoretical Background

In this chapter, we explain the theoretical background of surface plasmons, it's excitation methods, electrochemistry and ion-potential distribution in electrochemical cell in detail.

2.1 Surface Plasmon

Surface plasmons are free electrons which are oscillating paralel between the metal-dielectric interfaces. They generate electromagnetic fields thus they are called as electro-magnetic waves.

2.1.1 Surface Plasmons at Metal Dielectric Boundaries

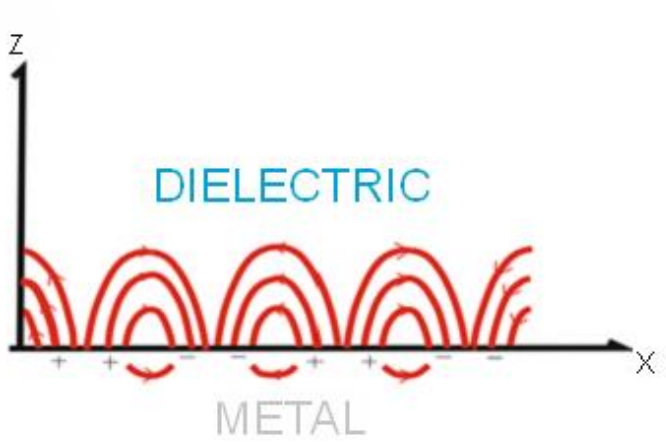

Figure 2.1: Surface Plasmons between metal,dielectric media

Changes in surface charge density provide electromagnetic field. Amount of the field depends on distance from the surface. It decreases exponentially in both media.

Surface plasmons mode is explained by Maxwell's equations. Assume that nonmagnetic media and ε does not change dramatically with distance,

$$\nabla^2 E - \frac{\varepsilon}{c^2}\frac{\partial^2 E}{\partial t^2} = 0, \qquad (2.1)$$

Due to the harmonic time dependence, we can write $E(t) = Ee^{-i\omega t}$ and put this into equation 2.1 and we obtain,

$$\nabla^2 E + k_o^2 \varepsilon E = 0, \qquad (2.2)$$

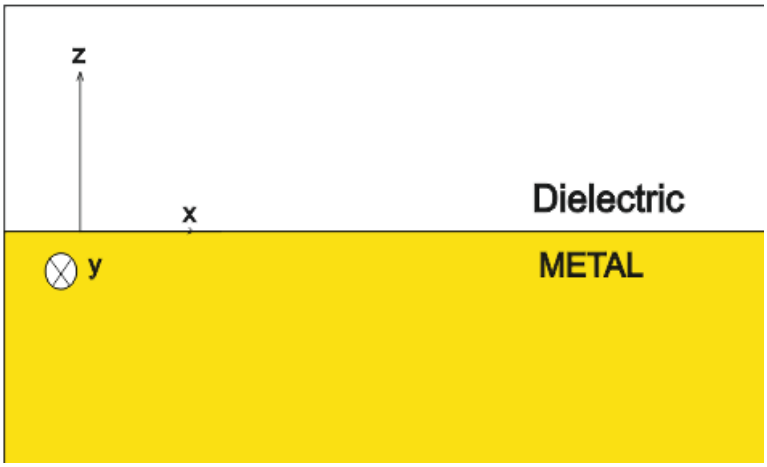

Figure 2.2: Geometry for wave propagation at a metal-dielectric interface

Considering such a propagation geometry as shown in Figure 2.2, ε is depending on only z-direction, wave propagates in x-direction and no variation in y axis $\left(\frac{\partial}{\partial y} = 0\right)$, wave equation of surface plasmon is $E(z) = e^{i\beta x}$, where β is propagation constant of surface plasmon in x direction. Then we put new wave equation into equation 2.2 and we get,

$$\frac{\partial^2 E(z)}{\partial z^2} + (k_o^2 \varepsilon - \beta^2)E = 0\,, \qquad (2.3)$$

This equation satisfy E field but we have H field as well. We need to make connection between these 2 components thus we use Maxwell's Curl Equations,

$$\nabla \times E = -\frac{\partial B}{\partial t}, \qquad (2.4)$$

$$\nabla \times H = J_{ext} \frac{\partial B}{\partial t}, \quad (2.5)$$

Propagation is along x-axis($\frac{\partial}{\partial x} = -i\beta$) and as mentioned $\left(\frac{\partial}{\partial y} = 0\right)$,

$$\frac{\partial H_y}{\partial z} = \omega \varepsilon_0 \varepsilon E_X, \quad (2.6)$$

$$\frac{\partial H_x}{\partial z} - i\beta H_z = -i\omega \varepsilon_0 \varepsilon E_y, \quad (2.7)$$

$$i\beta H_y = -i\omega \varepsilon_0 \varepsilon E_z, \quad (2.8)$$

$$\frac{\partial E_y}{\partial z} = -i\omega \mu_0 H_X, \quad (2.9)$$

$$\frac{\partial E_x}{\partial z} - i\beta E_z = -i\omega \mu_0 H_y, \quad (2.10)$$

$$i\beta E_y = -i\omega \mu_0 H_z, \quad (2.11)$$

We can solve these equations for p polarized (transverse magnetic) and s polarized (transverse electric) modes. Ex, Ez and Hy components are exist for TM mode whereas Hx, Hz and Ey are exist for TE mode. Then wave equation for Tm mode ,

$$E_X = -i \frac{1}{\omega \varepsilon_0 \varepsilon} \frac{\partial H_y}{\partial z}, \quad (2.12)$$

$$E_z = -\frac{\beta}{\omega \varepsilon_0 \varepsilon} H_y, \quad (2.13)$$

$$\frac{\partial^2 H_y}{\partial z^2} + (k_0^2 \varepsilon - \beta^2) H_y = 0, \quad (2.14)$$

Similarly for Te mode ,

$$H_x = i \frac{1}{\omega \mu_0} \frac{\partial E_y}{\partial z}, \quad (2.15)$$

$$H_z = \frac{\beta}{\omega \mu_0} E_y , \quad (2.16)$$

$$\frac{\partial^2 E_y}{\partial z^2} + (k_0^2 - \beta^2) E_y = 0, \quad (2.17)$$

As mentioned , evanescent decay occurs in z-axis. If we have Tm polarized wave propagating on the surface , for z>0 ,

$$H_y(z) = A_d e^{i\beta x} e^{-k_d z}, \quad (2.18)$$

$$E_X(z) = i A_d \frac{1}{\omega \varepsilon_0 \varepsilon_d} k_d e^{i\beta x} e^{-k_d z} , \quad (2.19)$$

$$E_z(z) = -A_d \frac{\beta}{\omega \varepsilon_0 \varepsilon_d} k_d e^{i\beta x} e^{-k_d z}, \quad (2.20)$$

Similarly for z<0,

$$H_y(z) = A_m e^{i\beta x} e^{k_m z}, \quad (2.21)$$

$$E_x(z) = -iA_m \frac{1}{\omega \varepsilon_0 \varepsilon_m} k_m e^{i\beta x} e^{k_m z}, \quad (2.22)$$

$$E_z(z) = -A_m \frac{\beta}{\omega \varepsilon_o \varepsilon_m} e^{i\beta x} e^{k_m z}, \quad (2.23)$$

Continuity should be provided (z=0) for H_y *and* E_x, by deriving equations 2.18 , 2.19 , 2.21 and 2.22 ,

$$A_m = A_d, \quad (2.24)$$

$$\frac{k_d}{k_m} = -\frac{\varepsilon_d}{\varepsilon_m}, \quad (2.25)$$

From equation 2.25 , k_d ve k_m are positive so one of the electrical permitivities is negative. This lead us that surface plasmons are exist while one media is insulator another is conductor. H_y must satisfied equation 2.21 , for z>0 and z<0 ,

$$k_m^2 = \beta^2 - k_o^2 \varepsilon_m , \quad (2.26)$$

$$k_d^2 = \beta^2 - k_o^2 \varepsilon_d , \quad (2.27)$$

Now we can introduce dispersion relation of surface plasmons, by inserting equation 2.25 into equation 2.26, and equation 2.27 ,

$$\beta = k_0 \sqrt{\frac{\varepsilon_m \varepsilon_d}{\varepsilon_m + \varepsilon_d}}, \quad (2.28)$$

We find dispersion relation of surface plasmon for Tm polarization now we drive the equations for Te polarization for the same geometry and z>0 ,

$$E_y(z) = A_d e^{i\beta x} e^{-k_d z}, \quad (2.29)$$

$$H_X(z) = -iA_d \frac{1}{\omega \mu_0} k_d e^{i\beta x} e^{-k_d z}, \quad (2.30)$$

$$H_z(z) = A_d \frac{\beta}{\omega \varepsilon \mu_0} e^{i\beta x} e^{-k_d z}, \quad (2.31)$$

Similarly for z<0,

$$E_y(z) = A_m e^{i\beta x} e^{k_m z}, \quad (2.32)$$

$$H_x(z) = -iA_m \frac{1}{\omega\mu_0} k_m e^{i\beta x} e^{k_m z}, \quad (2.33)$$

$$H_z(z) = -A_m \frac{\beta}{\omega\varepsilon\mu_0} e^{i\beta x} e^{k_d z}, \quad (2.34)$$

Continuity have to be provided for E_y , thus $A_m = A_d$, continuity also be provided for H_x , so $A_m(k_m + k_d) = 0$, k_d and k_m are positive , A_m must be equal to 0. It demonstrates that only Tm polarizated light can excite surface plasmons.

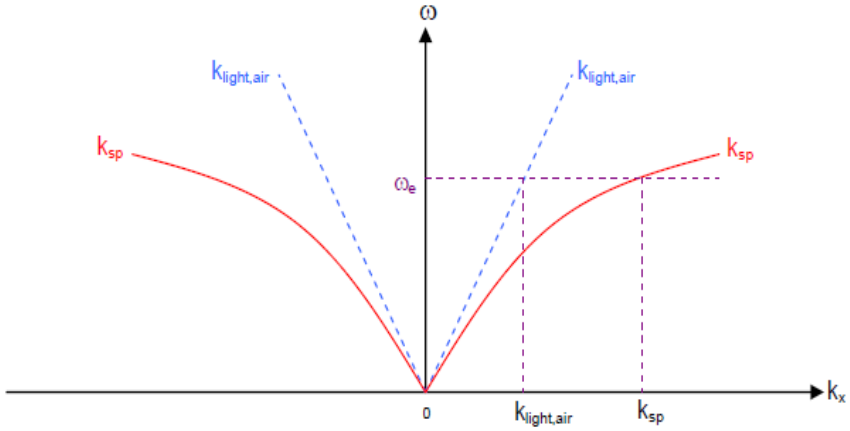

Figure 2.3: Dispersion relations between wavevector of light in air and wavevector of plasmon

In Figure 2.3 , no intersection between dispersion curves therefore direct excitation of surface plasmons is impossible.

2.1.2 Excitation Methods of Surface Plasmons

Excitation occurs when wave vectors of incoming light and surface plasmons are paralel. Incoming light transfers it's energy to the surface plasmons when excitation conditions meet. Dark bands are seemed at reflected light due to absorpted energy of incoming light. These bands are observed in terms of angle or wavelength of reflected light. These bands are also very sensitive to the surrounding of metallic media. Little changes in refractive index cause detectable movement at reflection spectra which has high potential for biosensor applications . As explained, direct

excitation is impossible, so different techniques must be used to excite surface plasmons. The most common methods are ; prism and grating coupling systems.

2.1.2.1 Prism Coupling

The most common method to excitation of surface plasmons is "Attenuated Total Reflection(ATR)" based prism coupling. The relation between dispersion equations of surface plasmon and light is;

$$\beta = k_0\sqrt{\frac{\varepsilon_m\varepsilon_d}{\varepsilon_m+\varepsilon_d}} \geq k_{pHoton} = \frac{\omega}{c}\sqrt{\varepsilon_d}\ , (2.35)$$

From equation 2.35 , momentum matching is not possible unless using high index prism since the prism increases k_{pHoton}. There are two types of prism coupling configuration; Kretschmann [27] and Otto geometry [28].

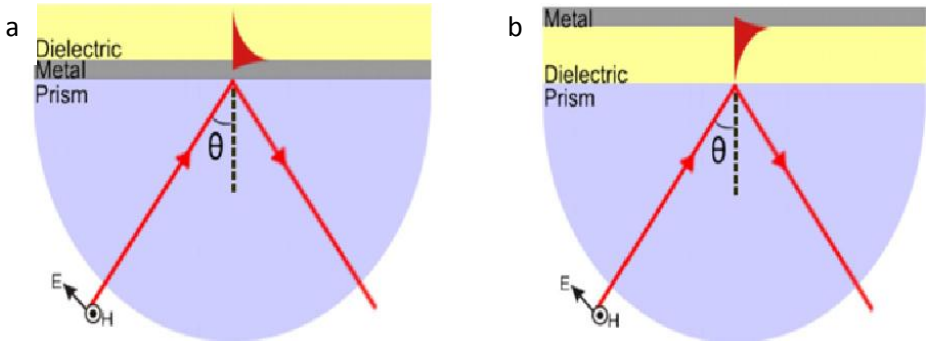

Figure 2.4 : Prism coupling geometry : (a) Kretschmann configuration , (b) Otto configuration

At Kretschman geometry, prism contacts directly with metal , while dielectric media contacts with prism at Otto geometry. Otto configuration is preferred where prism and metal conduction is unwanted. But the main problem of Otto configuration is addiction to the dielectric thickness of the system which is disrupted easily.

Kretschmann geometry is more common due to easy implementation and sensitivity. Light come into the prism and reflected from prism-metal interface but evenascently penetrates into metal. Excitation is performed by evenascent wave at metal-dielectric interface. During excitation, energy transfer takes place between

light and surface plasmon and changes in reflection spectrum in terms of wavelength or angle can be monitored.

2.1.2.2 Grating Coupling

Grating is explained as regular repetitation of periodic pattern. Periodic structure provides different diffracted orders. Incident light is diffracted into multiple orders with different diffraction angles. Excitation occurs when momentum of diffracted orders along the interface is equal to the momentum of surface plasmons. Assume that we have incident light with wavevector k_o and incident angle θ, horizantal wavevectors k_d of diffracted orders are;

$$k_d = k_o \sin\theta + m\frac{2\pi}{\Lambda} , \qquad (2.36)$$

m represents the diffraction order which is integer, ∧ is period of grating. From the equation 2.36 , wavevector of incident light can be improved with grating by changing incident angle of light and period of grating. As mentioned, momentums are must be equal so we can write equations for coupling condition as ,

$$\frac{2\pi}{\lambda} + m\frac{2\pi}{\Lambda} = \frac{\omega}{c}\sqrt{\frac{\varepsilon'_m \varepsilon_d}{\varepsilon'_m + \varepsilon_d}} , \qquad (2.37)$$

$$n_d \sin\theta + m\frac{\lambda}{\Lambda} = \pm\sqrt{\frac{\varepsilon'_m \varepsilon_d}{\varepsilon'_m + \varepsilon_d}}, \qquad (2.38)$$

Surface profile of grating has translational symmetry, so the plasmonic dispersion has also symmetry; therefore surface plasmons are excited both forward and backward directions . " ± " sign represents change in direction in equation 2.38. Therefore 2 splitted resonance dips shown at reflectance spectrum except 0^o angle of incident light. When 0^o angle of incident light, two resonances are overlapping and they seem as one. This condition is both advantage and disadvantage for several applications. For example, in biosensor applications, shift in resonance can be monitored from two dips and it provides double check in experimental results. But in filter applications, second unwanted filter may demolish experiments.

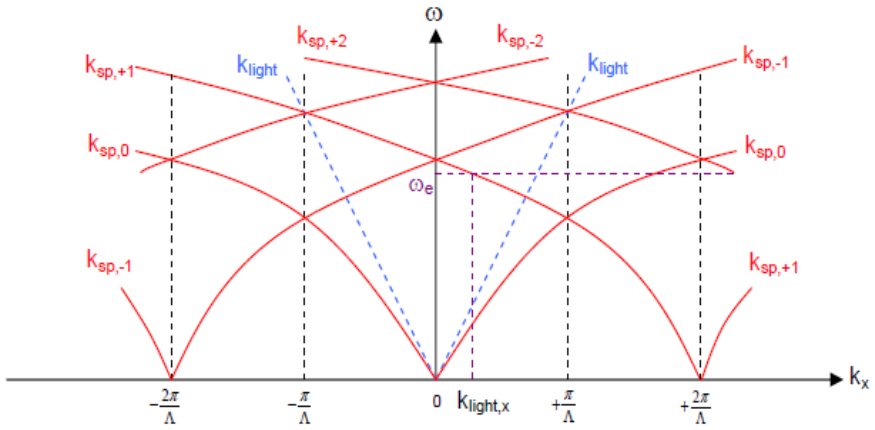

Figure 2.5: The plasmonic dispersion relation for grating coupling

Kretschmann configuration needs prism , costly equipments and large area and also studies about grating coupled method are low thus in this study we prefer grating coupling method to excite surface plasmons.

2.2 Electrochemistry

Electrochemistry is a branch of chemistry which is based on chemical reaction between electronic(metal v.s) and ionic conductor(electrolite). We call electrochemical reaction as if chemical reaction occurs by applying external voltage or voltage is produced by a chemical reaction.

In electrochemical reaction, electron transfer occurs between electrodes and electrolite. If the reaction ends with electron gain, it is called reduction and oxidaton is vice versa. Standart electrode potential of electrodes must be higher than ions in solution otherwise spontaneous reactions occurs.

Although gold, silver and aluminum are popular for plasmonic applications, aluminum is not appropriate for chemical applications due to it's chemically reactive properties.

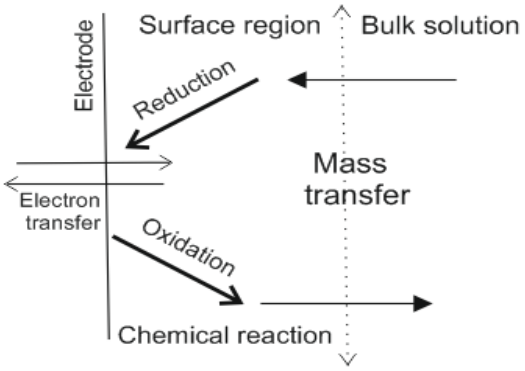

Figure 2.6 : Electrochemical reaction process

In ionic solutions, surface charges are equalized by counter ions in solution to preserve electrical neutrality. Several counter ions reduce on the surface and the others distribute in solution within the electrical double layer .

Assume that we have surface which is 1d planar and has constant potential ψ_0 , determined by number of ions on surface. The potential will decay with distance (x) and will be zero far away from surface. We can call the potential as a funtion of x; $\psi(x)$.

We can generaly describe the potential with poisson equation;

$$\nabla^2\psi_= \ -\rho^4/\varepsilon \ , \qquad (2.39)$$

ρ is charge density , ε is electrical permittivity. This equation is for three dimensions (3D) but our system is one dimesion(1d) therefore;

$$\frac{d^2\psi}{dx^2}= -\rho^4(x)/\varepsilon \ , \qquad (2.40)$$

ε is constant and boundary condition of the equation is ;

$$\psi(0) = \psi_o, \qquad (2.41)$$

$$\psi(\infty) = 0, \qquad (2.42)$$

Now we want to relate potential with the concentration of the ions in solution. We can explain that the ions in solution obey Boltzman distribution. Boltzman equation is ;

$$\frac{n_i}{n_{i,\infty}} = \exp\left(\frac{-z_i e\psi}{k_B T}\right), \quad (2.43)$$

Where n_i , number of ions per unit volume at ψ , $n_{i,\infty}$ concentration of ions in solution , e is charge of an electron , z_i is the valence of the ion , k_B is boltzmann constant and T is temperature. From equation 2.43 we can define charge density ;

$$\rho^+ = -z_i e n_i \, , \quad (2.43)$$

Now we have function relates charge density to potential distribution of the ions. If we have multiple ions in solution ;

$$\rho^+ = \sum z_i \, e n_i \; = \; \sum z_i \, e n_{i,\infty} \exp\left(\frac{-z_i e\psi}{k_B T}\right), \quad (2.44)$$

Now we have relation about charge density so we substituted back up into poisson equation and called Poisson-Boltzmann equation;

$$\frac{d^2\psi}{dx^2} = \frac{-e}{\varepsilon} \sum z_i \, n_{i,\infty} \exp\left(\frac{-z_i e\psi}{k_B T}\right), \quad (2.45)$$

No general solution to this equation unless some assumption. First assumption is surface potential is typically low , $-z_i e\psi \; << \; k_B T$. So we can linearize the equation;

$$\frac{d^2\psi}{dx^2} = \left(\left(\frac{e^2}{\varepsilon k_b T}\right) \sum z_i \, n_{i,\infty}\right)\psi \, , \quad (2.46)$$

if we call ,

$$K^2 = \left(\left(\frac{e^2}{\varepsilon k_b T}\right) \sum z_i \, n_{i,\infty}\right) , \quad (2.47)$$

K is kappa,then the equation is simply ,

$$\frac{d^2\psi}{dx^2} = K^2\psi, \quad (2.48)$$

This equation has a simple solution if we apply boundary condition;

$$\psi = \psi_0 \, e^{-kx} \;\; \text{or} \;\; \psi = \psi_0 \, e^{-x/k^{-1}} \, , \quad (2.49)$$

According to the equations, we explain potential and ion distribution in electrochemical cell.

CHAPTER 3

Characterization of Grating Structures

In this chapter , we analyz digital versalite discs(DVDs) to obtain grating structures by Atomic Force Microscopy(AFM). Then we simulate the grating structures by PC GRATE sofware to examine their plasmonic properties for different simulation parameters such as plasmon supporting layer , dielectric media and grating structure.

3.1 Characterization of grating structures

We explain the reason of usage of grating coupling method in previous chapter. Now it's time to supply grating structures. Commercially available DVDs has perfect fabricated and cheap grating structures so we decide to use DVD as grating mold. We observe surface topograhies of DVDs by AFM . AFM has 2 modes ; contact and tapping. In contact mode, AFM tips contact with surface and discover topographies of it with high resolution but tip or sample can be damaged at any moment. In tapping mode , we can discover surfaces without contact but of course with low resolution. By this way we reduce the possibility of damage in tip and sample . Our structures are not too small therefore we decide to use tapping mode.

We start AFM studies with Blueray discs becasue no information about these structures in literature thus this study will help researchers to uncover plasmonic properties of Blueray discs.

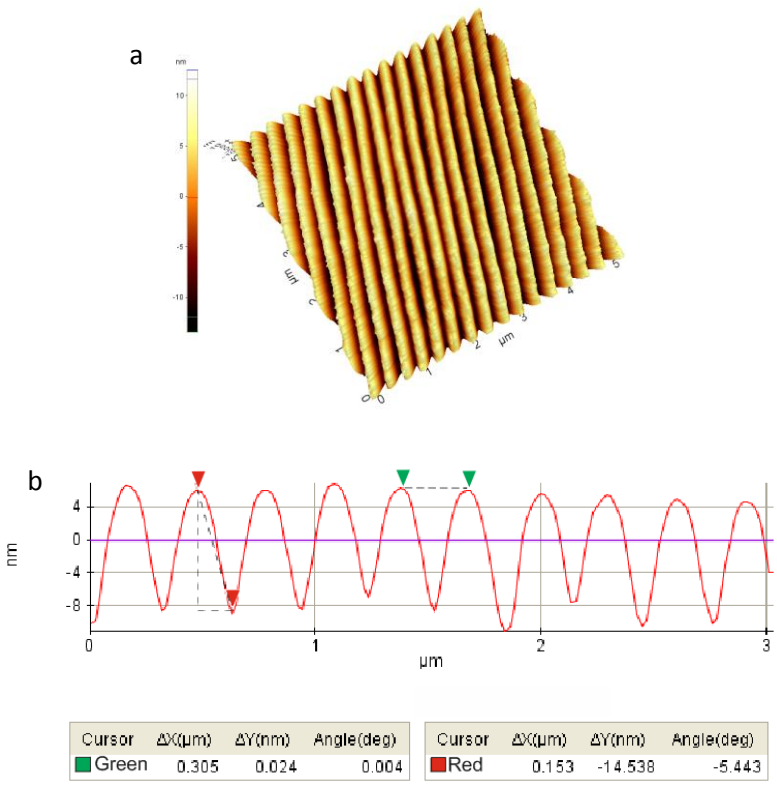

Figure 3.1: AFM image of Verbatim Blueray Disc ; (a) 3d surface topography, (b) Period and depth

According to AFM studies , we determine 15 nm depth and 305 nm period for blueray structure ,besides it seems like sinus trapezoidal(figure 3.1). The grating structures are smaller thus non-contact mode of AFM can not expose surface topography appropriately. Whereupon the period is repeated but the depth is not. Moreover blueray discs can not be easily availible in markets thus usage of blueray disc will problem to researchers who would use it in study. Also blueray discs are very costly, DVDs can be used as grating mold in applications but blueray discs can not under these conditions.

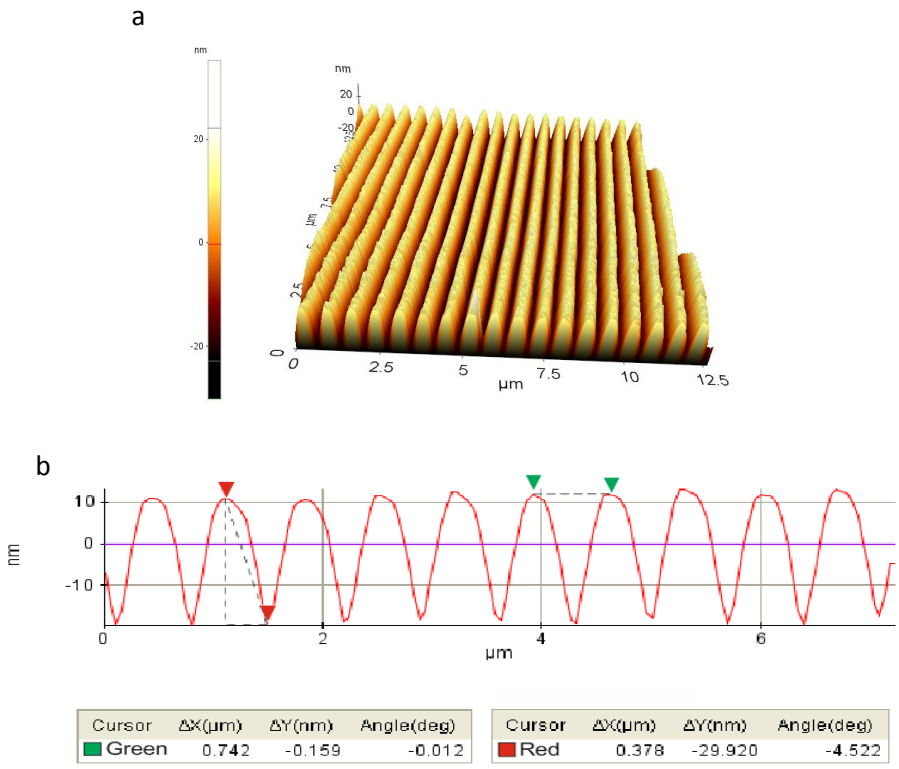

Figure 3.2: AFM image of Maxell Pro-x DVD ; (a) 3d surface topography, (b) Period and depth

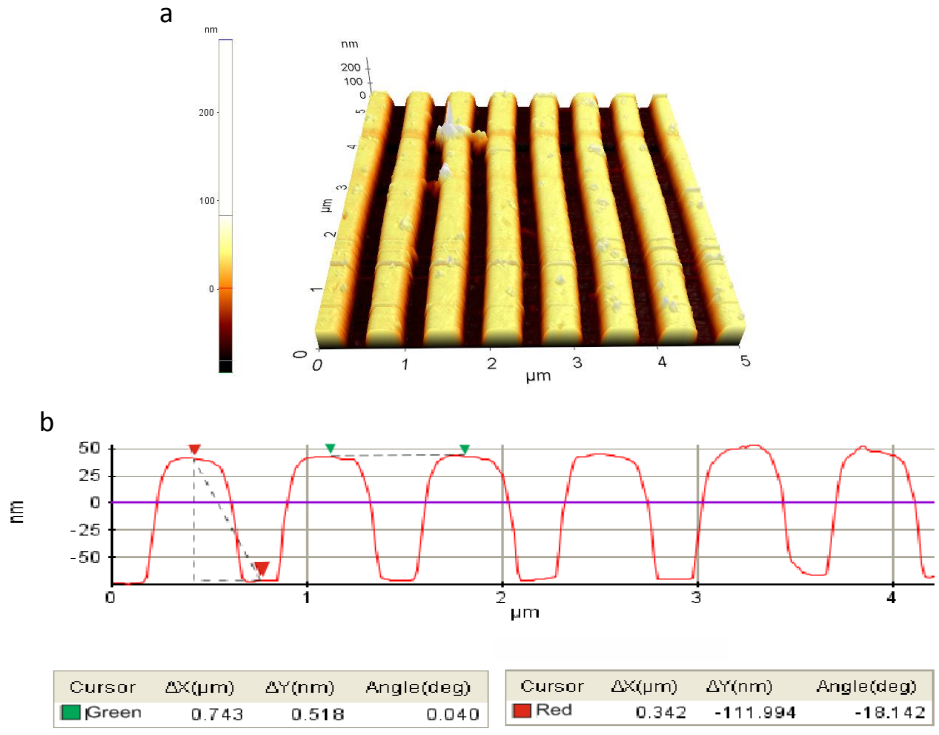

Figure 3.3: AFM image of Maxell R+DVD; (a) 3d surface topography, (b) Period and depth

According to the studies based on DVD grating structures, periods are common as 740 nm but depths are different thus we chategorize gratings in 2 groups ; namely Deep ve Shallow(Figure 3.2 and 3.3).

We investigate plasmonic properties of the gratings by numerical simulations. By this way , we observe the effect of incident light angle , different dielectric medias and plasmon supporting layers on the plasmonic properties of grating surfaces.

3.2 Numerical Simulations

In order to investigate plasmonic properties of the surfaces, we perform numerical simulations. We use PCGrate Version 6.5 software which provides different simulation parameters such as wavelength and angle of incident light. The grating structures are derived from AFM experiments.

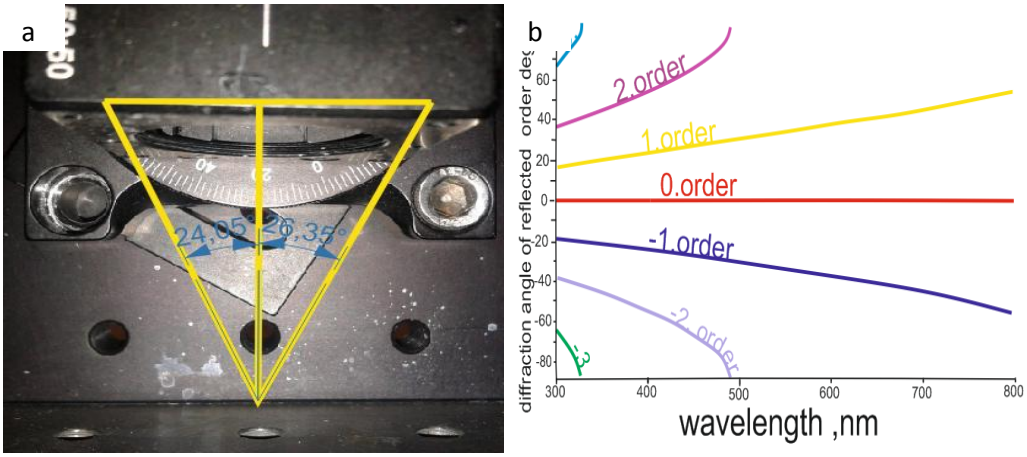

Figure 3.4: (a)Numeric aperture of experimental setup , (b) Diffraction Angle v.s Wavelength of Reflected Orders

The numeric aperture of the experiemental setup is 25^{o}. Simulations are performed on 0. reflected order since the other orders reflect with angles higher than numerical aperture of the experimental setup (Figure 3.4). We select gold(Au), Silver(Ag) and Aluminum(Al) as plasmon supporting metallic layer in simulations due to their plasmonic properties. Deionized water(DI water) is selected as dielectric media**.**

The most important parameter is defining grating structures appropriately while simulation. The structures are not defined properly and they will show differences in

experiments therefore we repeat AFM experiments multiple times to provide reliability As we observe, blueray discs grating structures are sinus trapezoidal. Edge profile of structures are defined by frequency of sinus function. Sinus frequency is determined as 2 hz because the edge profile of structures are not so sharp.

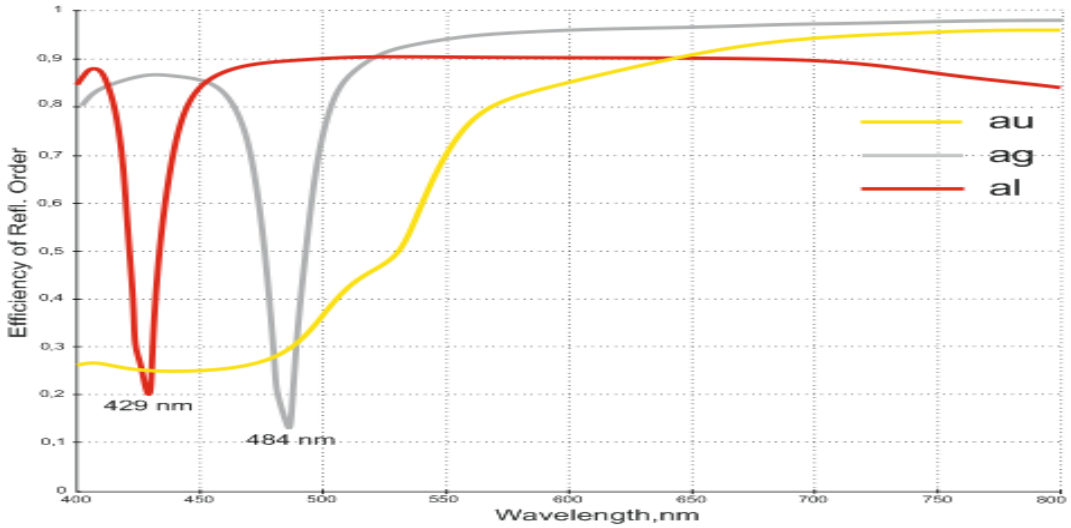

Figure 3.5: Wavelength interrogation simulation of blueray grating structure when DI water as dielectric media and Al, Au, Ag as plasmon supporting metallic layer

While DI water (n=1.33) as dielectric media, Al and Ag have sharp resonance profile thus we claim that these metallic layers are usable in plasmonic filter and biosensor applications.(Figure 3.5). But this is not valid for Au coated surfaces. While using blueray grating based plasmonic surfaces with 0^{o} incident light angle and DI water combination, useful results are impossible.

The second part of the simulations are performed on Shallow and Deep grating structures.

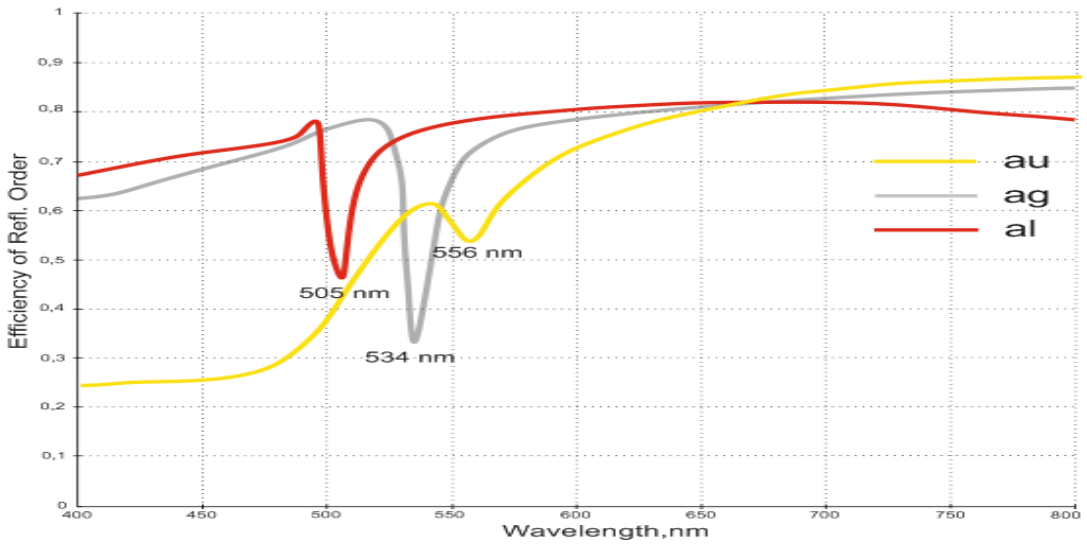

Figure 3.6: Wavelength interrogation simulation of Shallow grating structure when DI water as dielectric media and Al,Au,Ag as plasmon supporting metallic layer

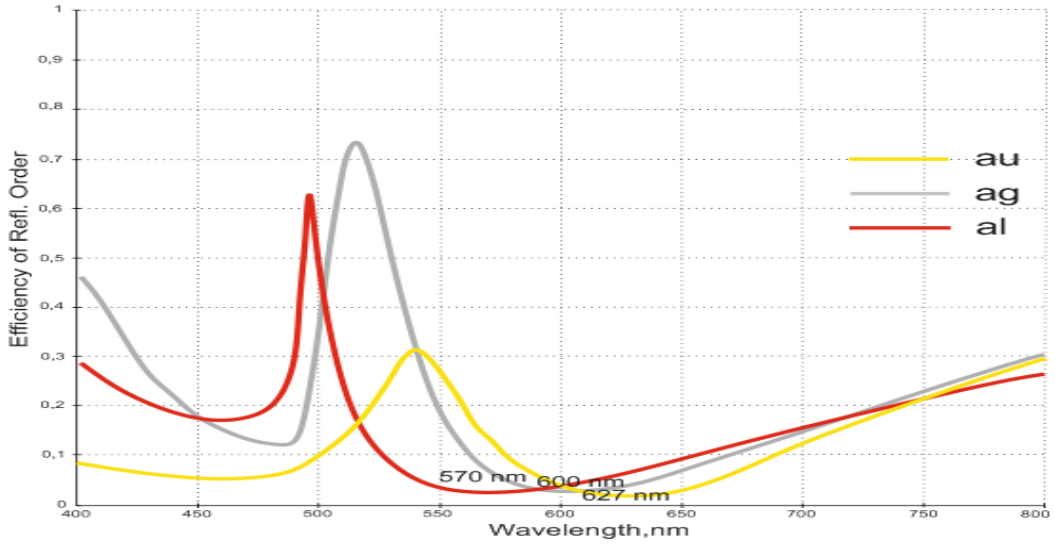

Figure 3.7: Wavelength interrogation simulation of Deep grating structure when DI water as dielectric media and Al, Au, Ag as plasmon supporting metallic layer

We study plasmonic properties of Deep and Shallow grating structures for different plasmon supporting layers. Shallow grating based plasmonic surfaces has sharp plasmon resonance, but when Au as metallic layer , no significant resonance profile is observed (Figure 3.7)

Plasmonic properties of Deep grating based surfaces open a completely different application area to us. Thanks to it's broad resonance profile , it behaves like band pass filter. Changes in refractive index can be detected in terms of color changing.

By this way, we can detect biomolecular interactions without costly equipments such as spectrometer. It can be used not only for sensing but also for imaging applications.

Thin layer blocks the electrochemical interaction with surfaces, hence contrast differences occurs between coated and uncoated parts. By this way, structures on surfaces can be monitored by camera. In Shan et al.'s study , they use prism coupling mechanism with ccd camera but according to the simulations, we can assert that this can be performed with grating coupled method and basic camera.

Up to now, we investigate plasmonic properties of DVDs by numerical simulations. After this time, we simulate to observe effect of copper nanolayer on plasmonic properties of plasmonic surfaces. We prefer copper for deposited material because we use copper sulfate solutions in experiments. We will explain why copper sulfate is selected as electrolite in further chapters.

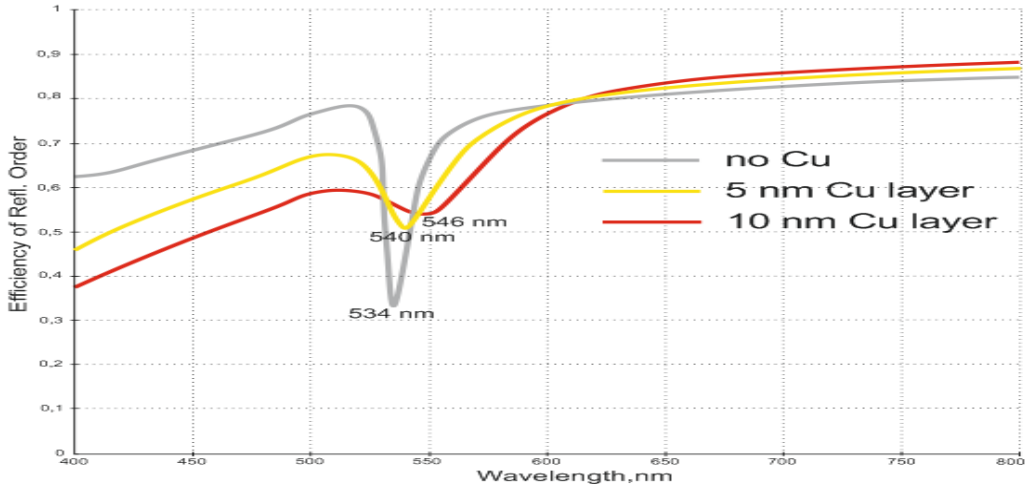

Figure 3.8: Wavelength interrogation simulation for different thicknesses of copper layer on Ag deposited surface when DI water as dielectric media

20 nm copper nanolayer shifts plasmon resonance almost 15 nm . On the other hand the thicker layer oblitirate plasmon resonance (Figure 3.8)

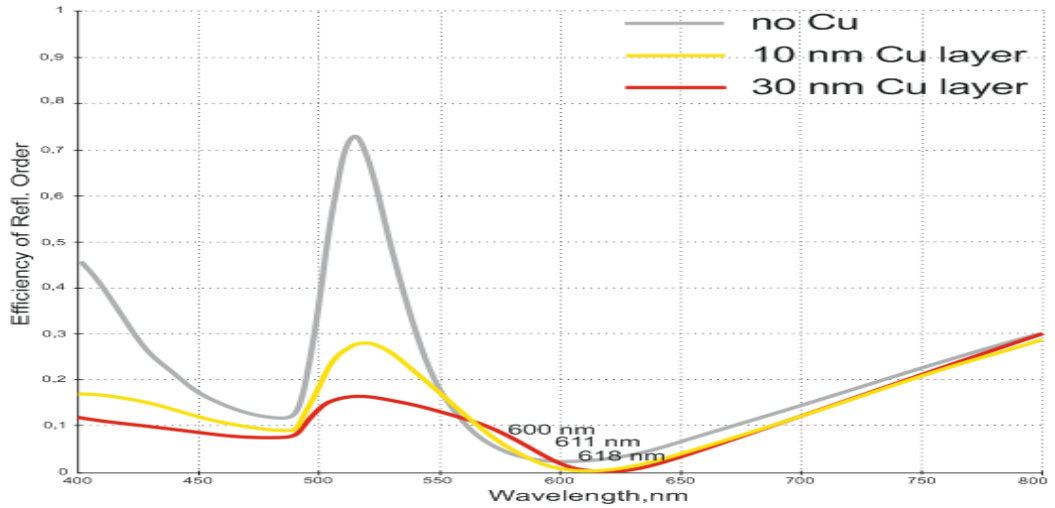

Figure 3.9: Wavelength interrogation simulation for different thicknesses of copper layer on Ag deposited surface when DI water as dielectric media

We observe the thin layer of copper shifted plasmon resonance for the both grating structures and thicker layer oblitirates it. By this way we theoretically demonstrate that plasmonic properties of surfaces can be controlled by electrochemically .Up to this time, simulations are performed with 0^o incident light angle but we need to investigate angle dependence of system. For this reason, we simulate the surfaces to observe effect of different angle

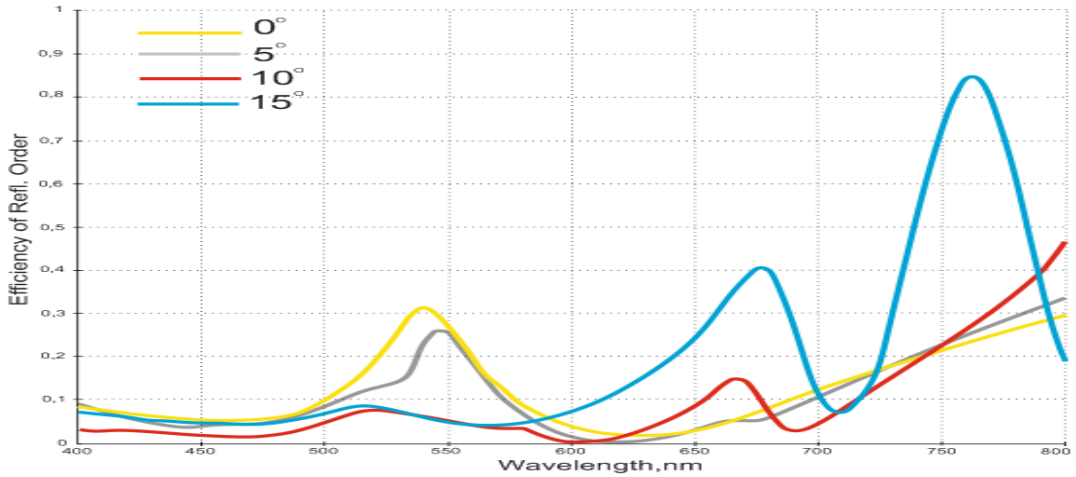

Figure 3.10: Angle interrogation simulation of Deep grating structure with different incident ligth angle; DI water as dielectric media and Au as plasmon supporting metalic layer

According to the angle interrogation simulations , our structures are highly dependent on incident light angle so we have to build optical experimental setup on 0^o incident light angle .

In summary, we investigate surface topographies of DVDs and blueray discs by AFM. We simulate grating structures for different plasmon supporting layer by PC Grate software. According to the simulation results, we observe that different grating structures have different plamonic properties. Especially Deep grating structures have great potential in SPR colorimetric sensing and imaging applications . After that we investigate effect of copper thin layers on plasmonic properties of surfaces. By this way, we demonstrate that plasmonic properties of surfaces can be controlled by electrochemistry. Finally we search the angle dependance of structures by numerical simulations. We determine that only experiments with 0^o angle of incident light can realized our expectations.

Chapter 4

Production

In this chapter, we explain the production of plasmonic gratings and electrochemical cell, preparation of electrolites and building of experimental setup in detail.

4.1 Plasmonic Gratings

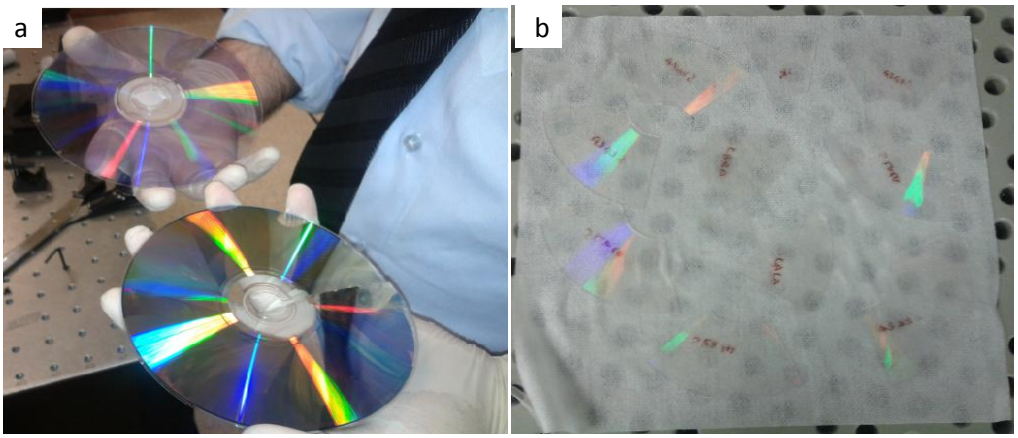

Figure 4.1: Sample preparation steps : (a) splitting it into 2 parts, (b) nitric acid threatment

We start with isolation of grating structures from DVDs. First, sample is cut with sciccors then splitted into 2 parts by hand. Nitric acid treatment is applied during 2 seconds to remove contaminations on sample (Figure 4.1) . Nitric acid treatment period is critical ; above 2 seconds , nitric acid damages the surface. After that 10 minutes ultrasonic cleaning is applied. We squeeze nitrogen on surface to dry. No need acetone treatment and also isopropanol should not be used. These steps must be carried on at clean room enviroment since the splitted parts are polluted easily which effects results dramatically.

For the requirement of plasmonic surfaces, we deposite metals on surfaces by thermal evaporator. Silver layer is damaged after electrochemical reactions, therefore we use germanium as adhesive layer. Although adhesive layer provides development, further improvements are needed. Higher coating thickness is better but sources of thermal evaporator should be used economically. According to our experiences, 60 nm metal thickness is sufficient to prevent transmittance of light and production of plasmonic surfaces. We keep coating rates below 0.5 angstrom / second for uniform coating.

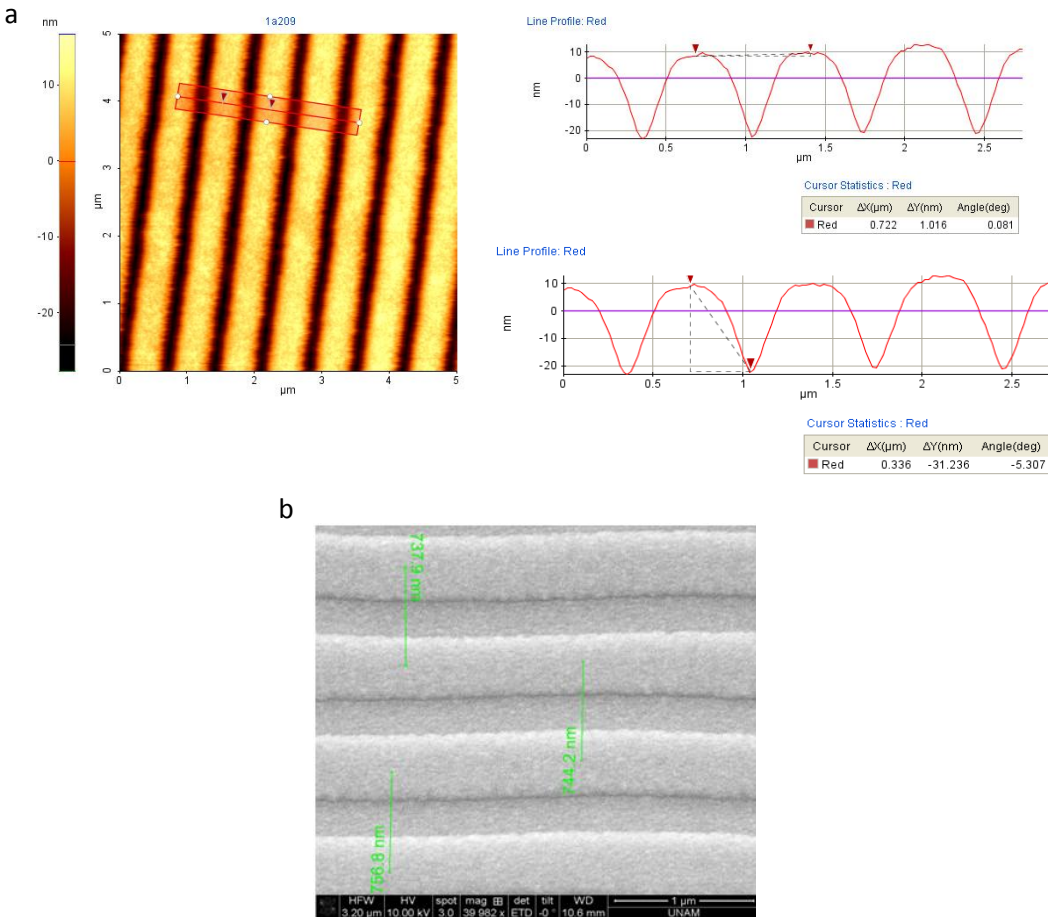

Figure 4.3: (a) AFM image of gratings after metal deposition (b) Sem image of coated sample

The grating structure of samples is protected in terms of period and depth (Figure 4.3). It demonstrated that the simulations are valid for the coated samples. Current regulation in thermal evaporator is also important. Fast changes in applied current causes sudden fracture on thermal evaporator boat. Rotation speed of sample must be optimized for uniform coating. Materials have high melting point such as

germanium are also problem. Boat can resist high temperature and current must be selected appropriately according to the coated materials.

The gratings produced are analyzed in terms of structure and purity by AFM and X-ray photoelectron spectroscopy (XPS). XPS is spectroscopic technique that indicates existance of elements within a material. X-ray stimulates surface and XPS simultaniously measures kinetic energy and number of scattered electron in range 10 nm to surface. Range is small and number of scattered electron is important therefore high vacuum condition is mandatory [29].

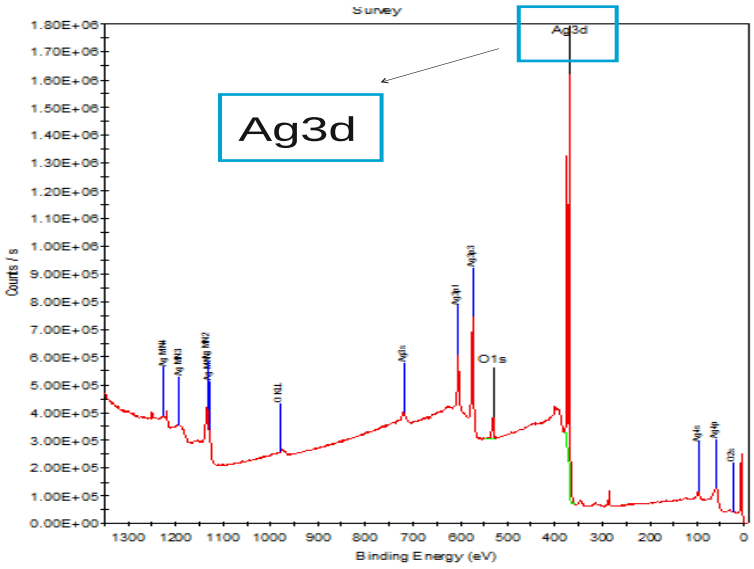

Figure 4.4 : Xps image of sample : survey analysis

Survey search reveals the existance of Ag on surface as well as no contamination(Figure 4.4). Now we sure that silver deposition is realized properly.

4.2 Electrochemical Cell

We start to create electrodes. First, we use shadow mask to split electrodes. But we can not adjust size of shadow mask appropriately thus big amount of sample is lost. For this reason, we deposite metal on DVD and split electrodes by tweezer. But the electrodes should be splitted properly by tweezer and conduction test must be performed by multimeter.

Conduction with electrodes is the most problematic part of the system. We start with silver pen which is liquid phase of silver but not good option due to following reasons;

- Poisinous ;gas mask have to be wear while using,
- Have to wait at least 30 minutes to dry
- Need conductive base

Second option is neomidyum magnet which provides good probing forwhy;

- Easy implementation
- Low resistance between probes and electrodes

Figure 4.6: First version of electrochemical cell

After conduction problem is solved, we start to product electrochemical cell. We cut 2 same size glass epoxy parts and open 2 screw holes to each other to provide pressure by screw. We put elastic ring between part and sample to determine height and width of the channel. Then we open 2 small holes and placed small pipes for tubing (Figure 4.6). Unfortunately we can not solve the bubble problem. Therefore we design new channel according to the problems. Samples bent after cutting and scraptining procedure thus we use glass wider than sample as basement and double-sided band as fixing material. On the other hand neonidyum magnets are used in

both conduction and fixing material on tables which are magnetized such as optical tables. The following steps are performed during production of electrochemical cell;

1. We cut appropriately sized piece from coated sample

2. We scrapt small area at middle of the sample to create electrodes by tweezer and check with multimeter that no conduction

3. We take wider glass than sample and use double-sided band to fix sample on the glass properly.

4. We cut appropriately sized piece from double-sided band and open a hole at middle of it by punch to fix channel onto the sample. The double-sided band also blocks solution which protrudes from channel

5. We place magnet at the edges of electrodes

6. We put small glass piece onto the channel to flatten bending

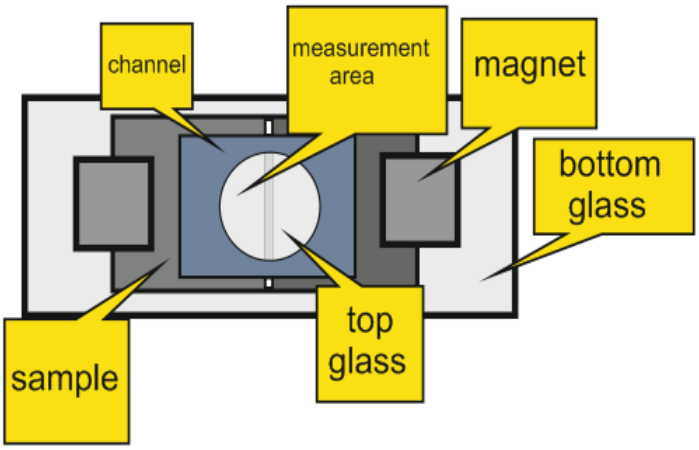

Figure 4.7: Final version of channel

By production of new electrochemical cell, we solve both the conduction and bubble problems. We create easily and quickly electrochemical cells by optimization of production process.

4.3 Experimental Setup

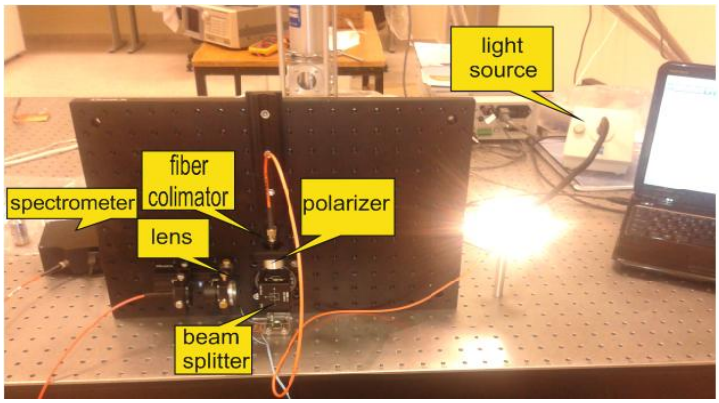

Figure 4.8: Optical experimental setup

We can not use ellipsometer because light is sent and collected with 0^o. Thanks to building of optical experimental setup by ourselves, we have mobile and easily adaptable system. We provide broad band light with gaussion distrubution from Zeiss light source . We carry light to the fiber colimator by fiber optic cable. Fiber colimator parallelizes light and we adjusted polarizer to change polarization of parallelized light. Beam splitter lets us sending and collecting light at the same time. We use lens to focus light to the fiber optic cable. The fiber optic cable carry light to the spectrometer (Figure 4.8) . Thanks to carrying light with fiber optic cable, light source and spectrometer can be changed easily. By this way, we can work in full range of light. After a while, we change the spectrometer with camera for imaging applications in further experiments.

4.4 Electrolites

We mention that plasmonic properties can be controled by electrochemistry. For this purpose, we prepare copper sulfate(CuSO4) solution as electrolite due to copper's reduction potential which is lower than silver and gold. Solid copper sulfate is supplied from Merck Industry. Solutions with different concentrations are prepared by AND GR200 precision weighning balance. According to the reduction potential of eletrode, different solutions can be prepared to perform different experiments. But copper sulfate is easily available and coherent with Au and Ag so we prefer it as electrolite. We prepare copper sulfate solutions with different molarities to observe effect of different concentrations on plasmonic properties.

CHAPTER 5

SPR and Electrochemical Experiments, Lumerical Simulations

In this chapter , we perform SPR experiments to investigate plasmonic properties of surface for different grating structures and plasmon supporting metallic layers. Cyclic voltagram experiments are performed to investigate redox reactions of copper. Finally we use Lumerical software to simulate copper nanoislands with different heights and densities on plasmonic surfaces.

5.1. SPR Experiments

After production process , we perform SPR experiments to observe coherence between simulations and samples. By this way , we determine the differences and it's reasons. We perform experiments not only for DI water but also for air as dielectric media. Experiments are performed with 0^o incident light angle as explained in previous chapter. But we don't carry out with different angles of incident light , it may be performed in future to observe angle dependence of the systems. We explain in chapter 4 that we split DVDs into 2 parts but the simulations are performed for one. But here, we perform the experiments for the other side and investigate the important parameters of surface plasmon resonance by comparing results.

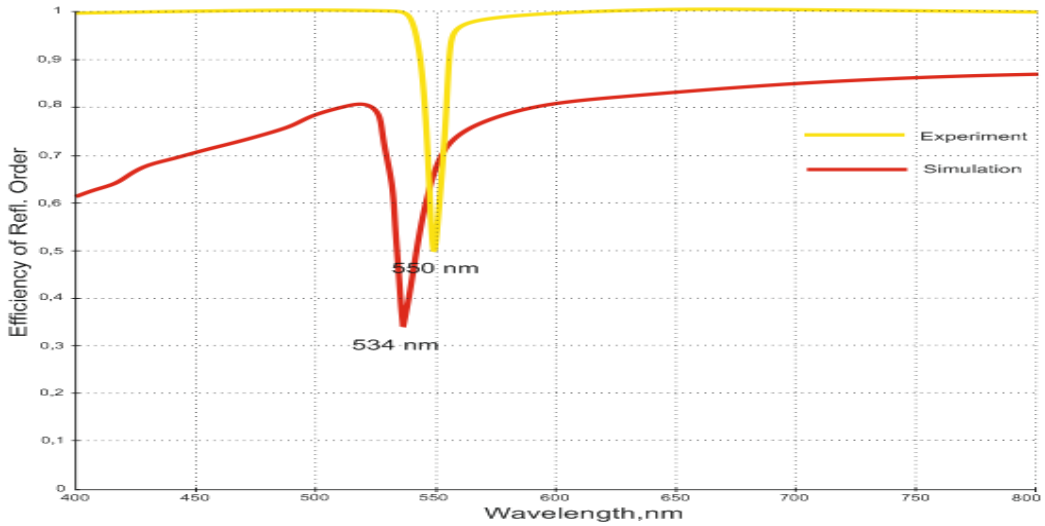

Figure 5.1 : Reflection spectrum of Shallow grating structure when 60 nm silver on 10 nm germanium as metallic layer, DI water as dielectric media

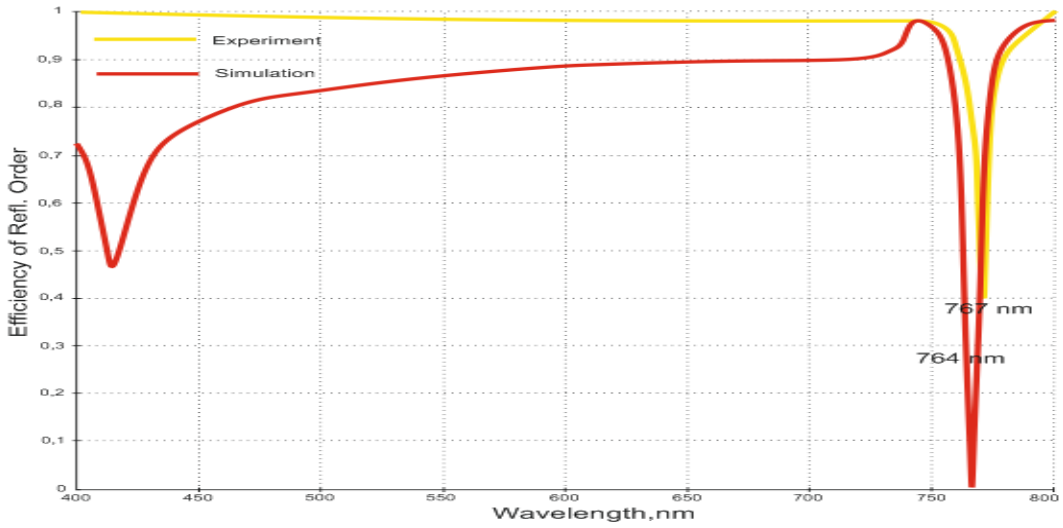

Figure 5.2 : Reflection spectrum of Shallow grating structures when 60 nm Ag over 10 nm Ge as metallic layer, air as dielectric media

As you can notice from experiments based on silver surfaces, the results are coherent with the numerical simulations(Figure 5.2). By this way , we check both accuracy of simulations and production process. Sensitivity is calculated as 0.00660 refractive index unit(RIU) which is coherent with literature[30].

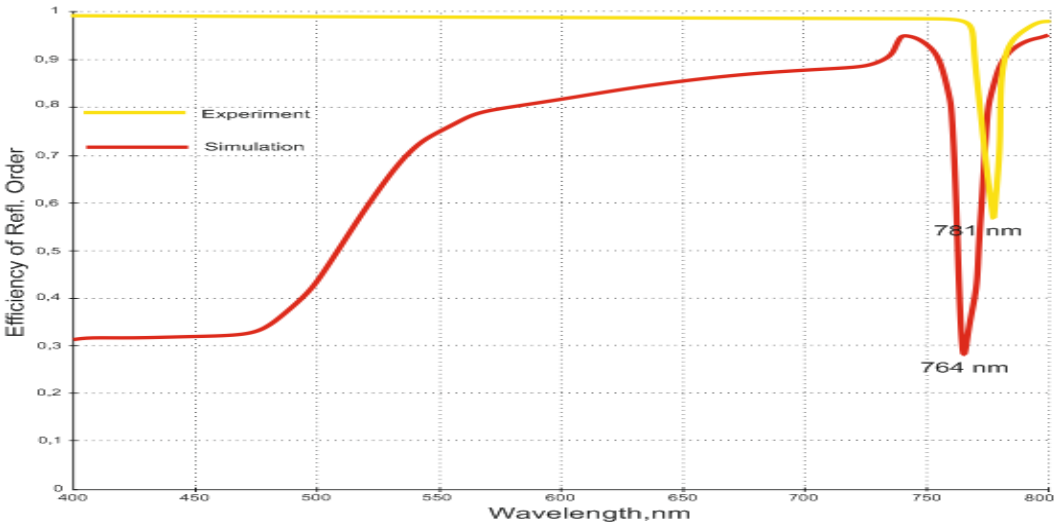

Figure 5.3 : Reflection spectrum of Shallow grating structure when 60 nm gold as metallic layer, air as dielectric media

We do not observe significant resonance profile for golden surace while DI water as dielectric media which is coherent with simulations. The coherence between simulations and experiments for the golden surface proves that structures can be applied in various metals. But as we mention, 0^{o} incident light angle with Shallow grating and DI water combination is not suitable. Maybe experiments with different angles can provide usable combinations.

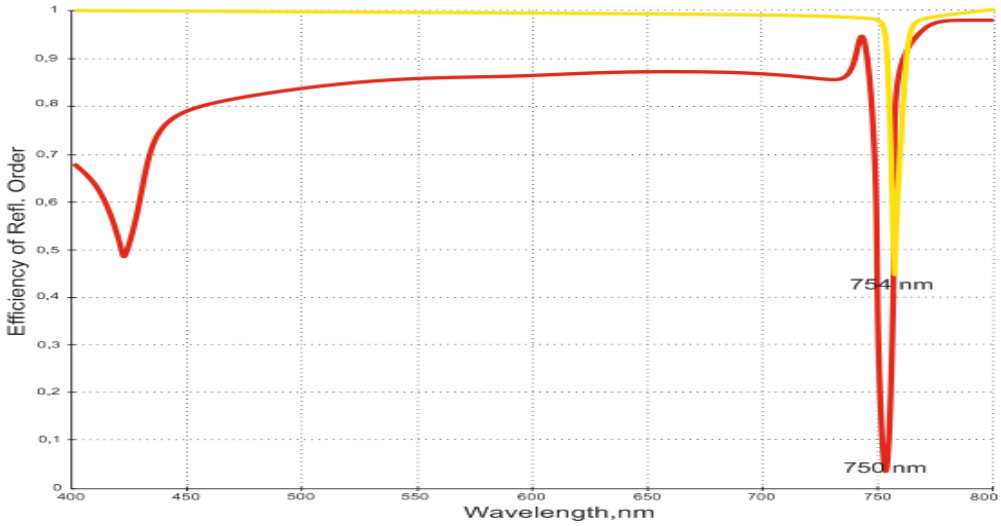

Figure 5.4 : Reflection spectrum of Shallow grating structure(other side of DVD's) when 60 nm silver over 10 nm germanium as metallic layer, air as dielectric media

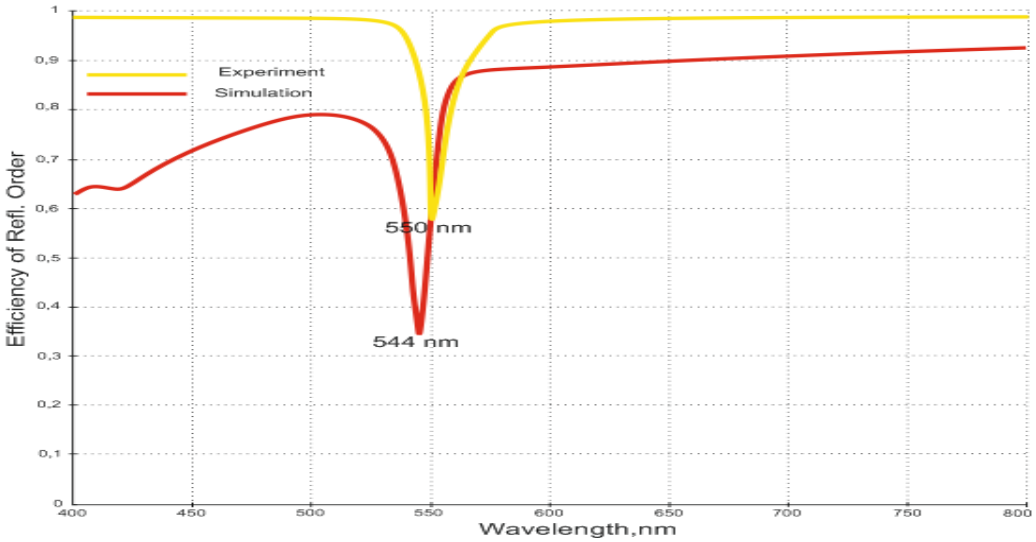

Figure 5.5 : Reflection spectrum of Shallow grating structure(other side of DVD's) when 60 nm Ag over 10 nm Ge as metallic layer, DI water as dielectric media.

As you can notice, simulations and experiments are coherent(figure 5.1, 5.2, 5.3, 5.4 , 5.5). The sensivity of surface is 0.00618 RIU which is almost equal to other side's sensitiviy which demonstrates that both splitted parts can be used as grating mold.

In summary, experiments with Shallow gratings are coherent with simulations. By this way, we demonstrate that both sample production and simulations are performed properly. The experiments with the other part of the DVD allow us to determine that both sides of the DVD can be used for experiments, thus one DVD would provide samples as much as 2 times. In addition, the cost for a mold can be reduced half. Fabrication would be possible by making functionalization of surfaces of DVDs even without producing our own mold. These experiments show that duty rate of grating structure does not alter the resonance profile but shifts the resonance point. In this way, we observe that adjustment can be made by only adjusting duty cycle without manipulating the depth and period of the structure in applications where it is critical to make a specific adjustment to the resonance point . Center position of the filter can be adjusted in this way in plasmonic filter applications.

Since Shallow grating experiments are available in the literature, we perform the experiments only with air and DI water; however we consider appropriate to use mixture of glycerol and DI water in order to perform experiments in more detail

because the Deep grating is a new structure and has interesting properties. We adjusted glycerol to DI water ratio in order to achieve precision refractive indexes. Ratios are given by weight. n represents refractive index of glycerol-DI water solution. Silver is used as plasmon supporting metallic layer. Volumetric ratio is used to adjust the glycerol to water. As the volume of liquids is known, the weight is calculated by using their density so we determine refractive indexes on the weight-refractive index table (table is not here).

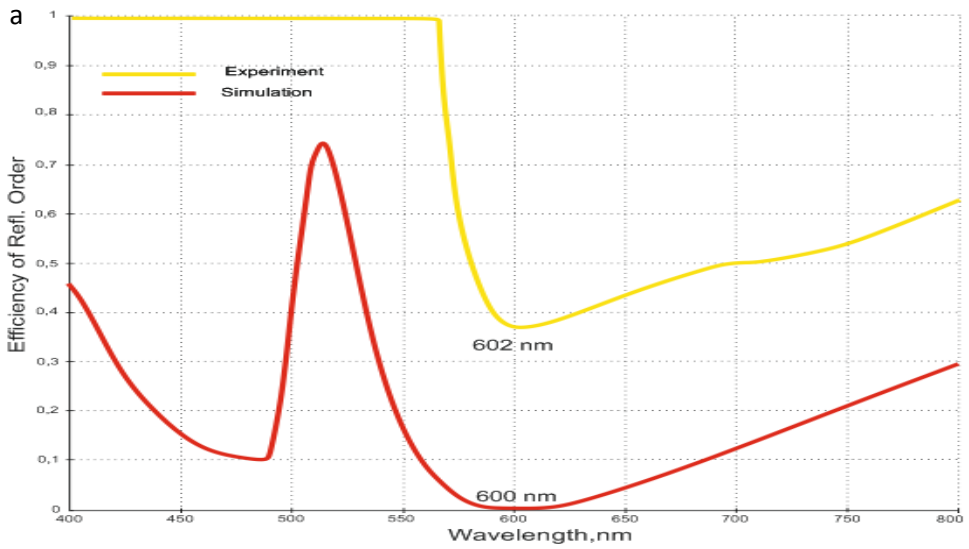

Figure 5.1: Reflection spectrum of Deep grating structure when %100 DI water(n=1.33) as dielectric media

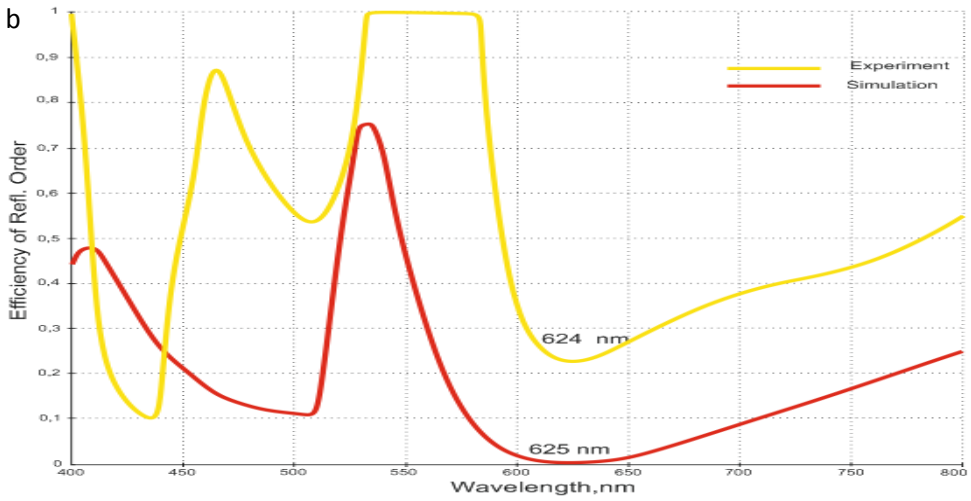

Figure 5.2: Reflection spectrum of Deep grating structure when %36 glycerol solution (n =1.3787) as dielectric media

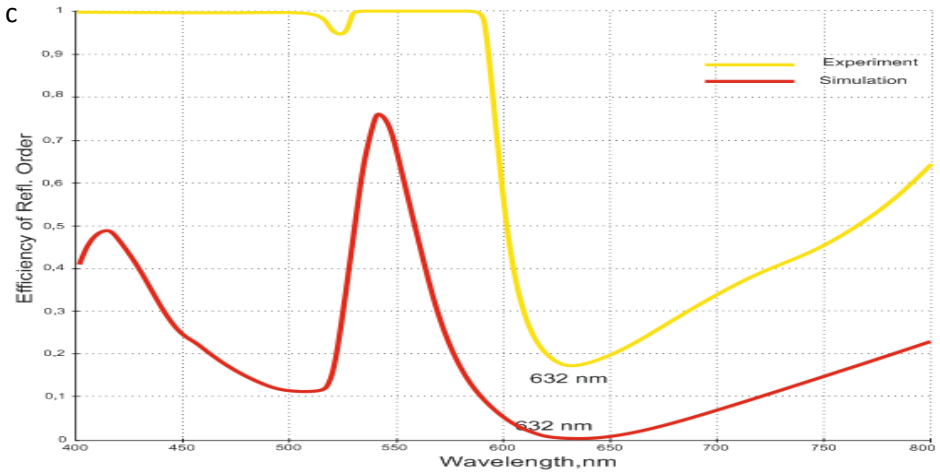

Figure 5.3: Reflection spectrum of Deep grating structure when %53 glycerol solution (n=1.4025) as dielectric media

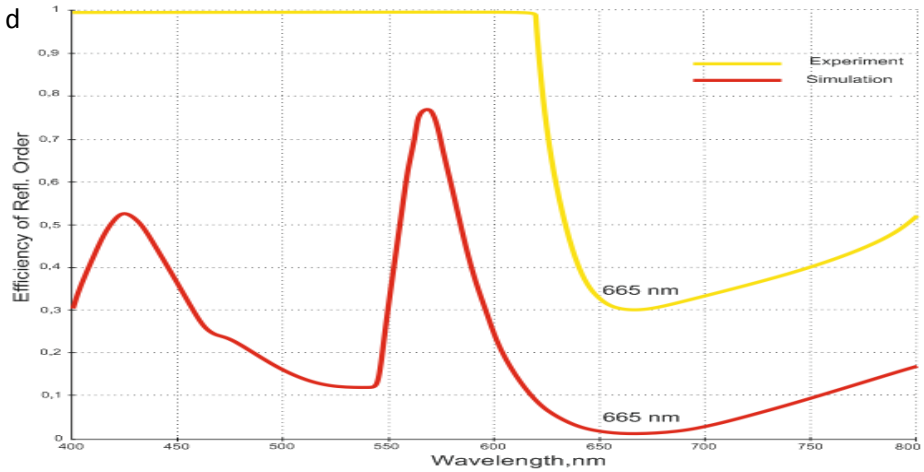

Figure 5.4: Reflection spectrum of Deep grating structure when %100 glycerol (n=1.47399) as dielectric media

The results from the experiments performed on Deep grating based plasmonic surfaces are fully consistent with the simulations. Based on the glycerol testing, a shift of 60 nm is achieved in resonance thus we observe occurrence of color change we mention. On the other hand, we calculate the sensitivity of Deep grating structure as 0.00458 RIU (Figure 5.6). The results of sensitivity have been proven to use readily in biosensor applications. Detection of biomolecular interactions with SPR based color change makes this grating structure different from other structures. With this system, it is possible not only analyze the interaction but also obtain imaging as mentioned before. In addition to plasmonic properties of this structure, it's tolerance against small misalignment in the optical measurement setup offers another reason to

use. It is possible to perform Shallow based grating studies with perfect alignment of optical mechanism but this structure relieves us such necessity.

In summary, as a result of SPR experiments performed with Deep and Shallow grating structure , we observe that the samples prepared and the optical setup are proper; simulations are performed correctly; the systems give correct results not for only one grating structure but also for different grating structures and are consistent with simulations in different metallic layers. After that point, if electrochemical reactions are properly controlled, we prove that plasmonic properties of the surfaces can also be controlled; filtering is possible with Shallow grating whereas colorimetric sensing and imaging is possible with Deep grating structure.

5.2 Cyclic Voltagram

In previous sections ,we demonstrate that changing refractive index of dielectric media shifts resonance wavelength for both grating structures . Now we assert that if we control refractive index of surface by deposition and stripping, we produce electrochemically switchable plasmonic surfaces. For this purpose , we perform cyclic voltagram experiments for copper sulfate solutions with different concentrations to investigate redox reactions of copper.

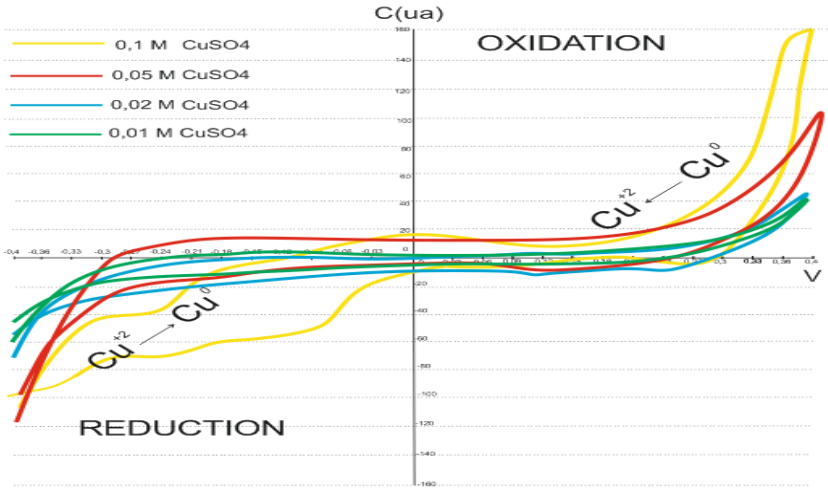

Figure 5.10: Cyclic voltagram of 0,05 M CuSO4 solution between ±0,4 V

Although the cyclic voltammogram range of copper sulfate solutions is ±0.5 volt in the literature, we show that 0.5 volt damaged the silver surface. We therefore keep

the voltage range at ± 0.4 volt. We observe that copper on the surface is stripped and converted into ions in the solution as gradually increased to "+ "voltages whereas the ions in the solution deposited on the surface as "–" voltages applied (Figure 5.7). We also witnessed that this repeated for different molarities. Reaction currents increase with high molarities but evenly deliver uncontrolled current responses. We can say that it is because not only increased concentration but also the system with 2 electrodes. We also suggest that the systems with a constant current, not a constant voltage, would improve the system's stability. With these experiments, we demonstrate that ± 0.4 volt guarantees reduction and oxidation for solutions in different concentrations. We therefore decided to use a constant voltage. Thus, we can easily and quickly control the reactions without the need for an adjustable power supply. Precision control of the reactions is not our primary purpose. But we intend to include precision control of redox reactions in future studies. After experiments , use XPS to discover what material is deposited on the surface; if it is copper that adhered to the surface; whether any undesired depositions occur in addition to copper.

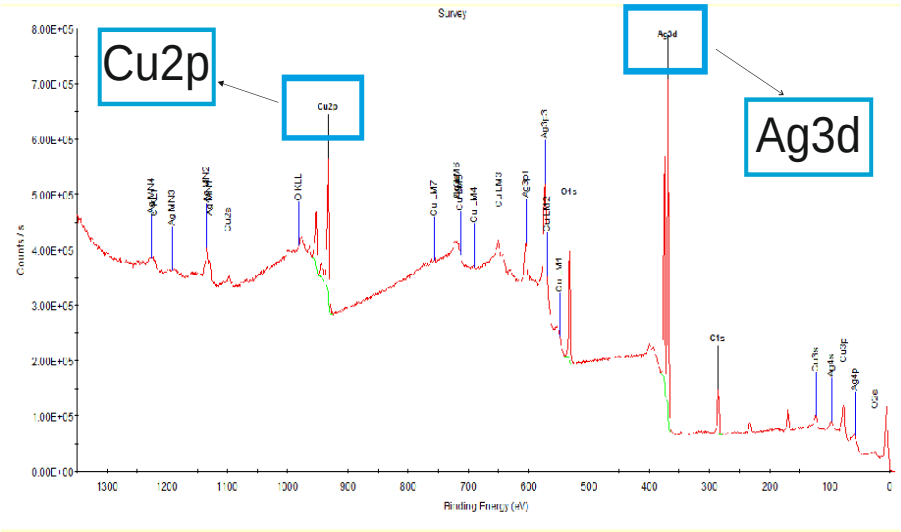

Figure 5.11 : XPS result after cyclic voltagram

Based on the XPS results, we prove that there are copper and silver on the surface; no undesired reactions occur thus the reactions are totally under our control.

After demonstrating we can control the reactions electrochemically, there is only one unknown matter left. We show in simulations that copper is coated on the

surface as a thin film, therefore plasmonic properties are changed; but we do not yet performed any studies on in what formation copper deposited on the surface. We therefore examine the samples. We apply constant voltage in different periods and determine copper formation on the surface and its alteration in time by SEM.

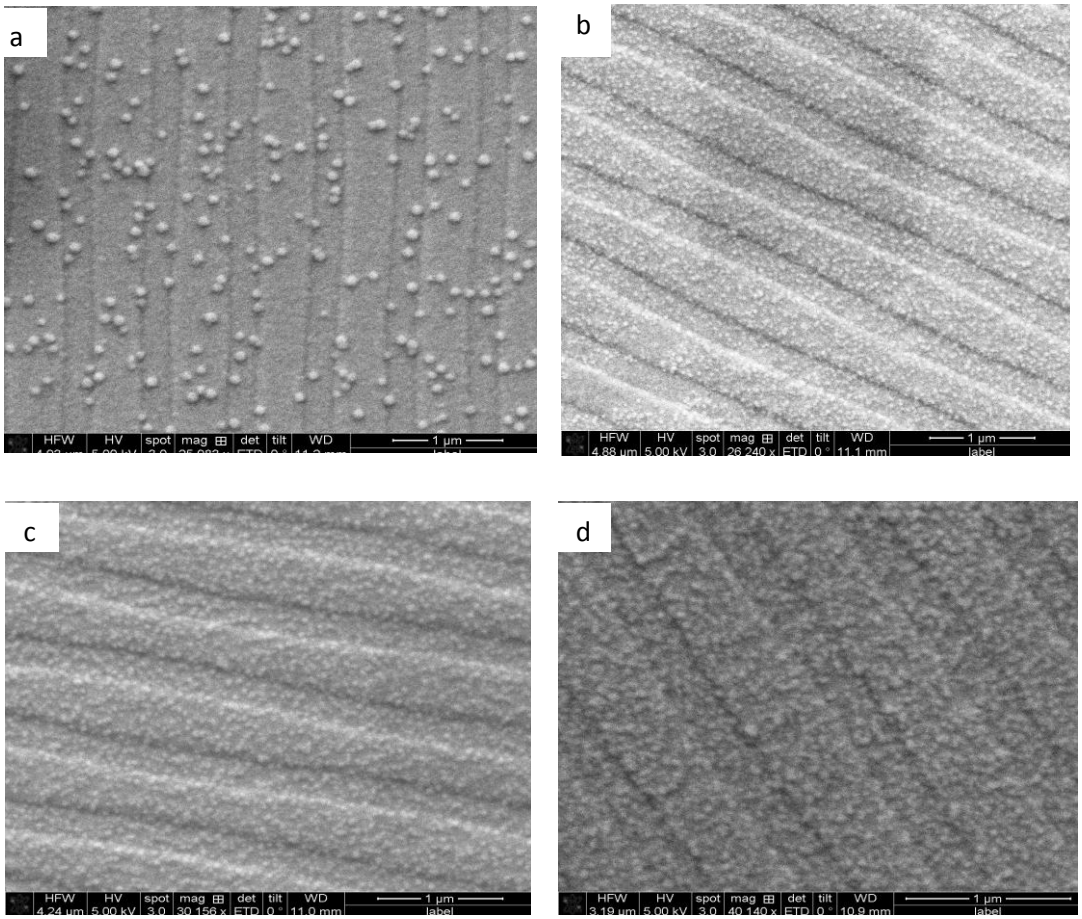

Figure 5.12: Sem image of silver coated grating surface with 0.05M CuSO4 solution after applying -0,4 volt during ; (a)3 seconds , (b)7 seconds, (c)10 seconds, (d)15 seconds

The copper deposits on the surface in copper nano islands not in thin film. In addition, density of copper nano islands increases as the time of application is increased.(Figure 5.9) The simulations performed in previous chapters are based on the reduction of copper to the surface as a nano layer; however we observe after the last study that is not true then perform simulations to see the effects of copper nano islands on plasmonic properties of the surfaces.

5.3 Lumerical Simulations

Because PC grate program is not developed enough to perform such a simulation, we use the Lumerical Program, a stronger simulation program, to examine the change in plasmonic properties depending on copper nano islands. With Lumerical Program, we determine how not only optical properties but also electrical and magnetic fields are confined on the surface and surrounding. So, we can observe plasmonic properties of grating structures in more details. Simulations are carrid out on Deep grating profile with silver as plasmon supporting metallic layer.

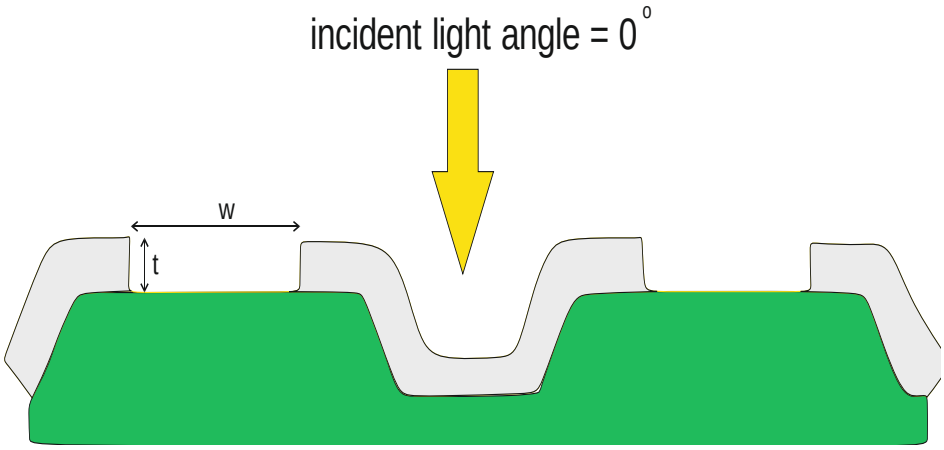

Figure 5.13: Simulated grating structure by Lumerical software

We use the structure above to simulate effect of copper nanoislands on plasmonic properties of surfaces. Here, w represents width of periodically empty area and t is thickness of copper thin film.(Figure 5.10) We change w and t in simulations to represent copper nanoislands have different lengths and thicknesses. Thus, we have the opportunity to witness how plasmonic properties changed depending on the change in effective copper thickness.

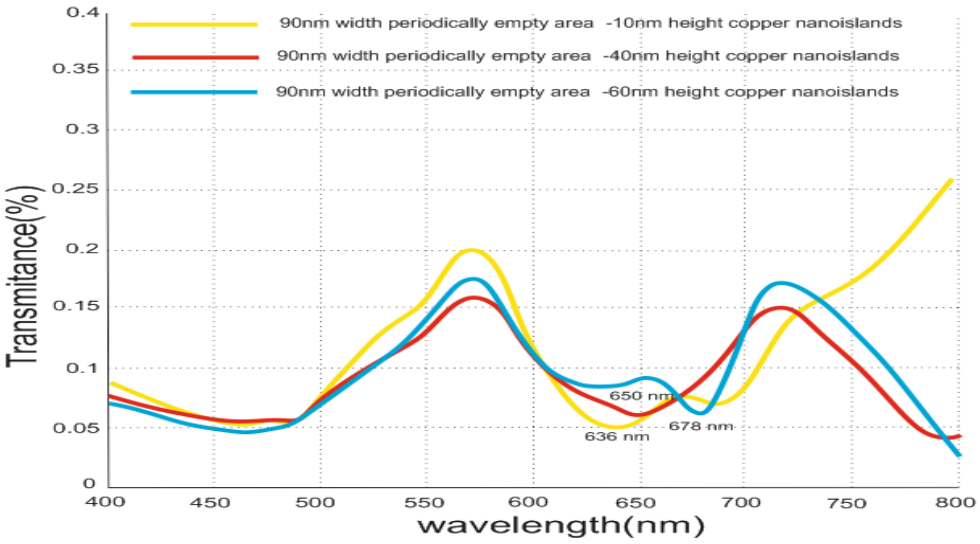

Figure 5.14 :Simulation for 90 nm width periodically empty area with 10,40,60 nm height copper nanoislands

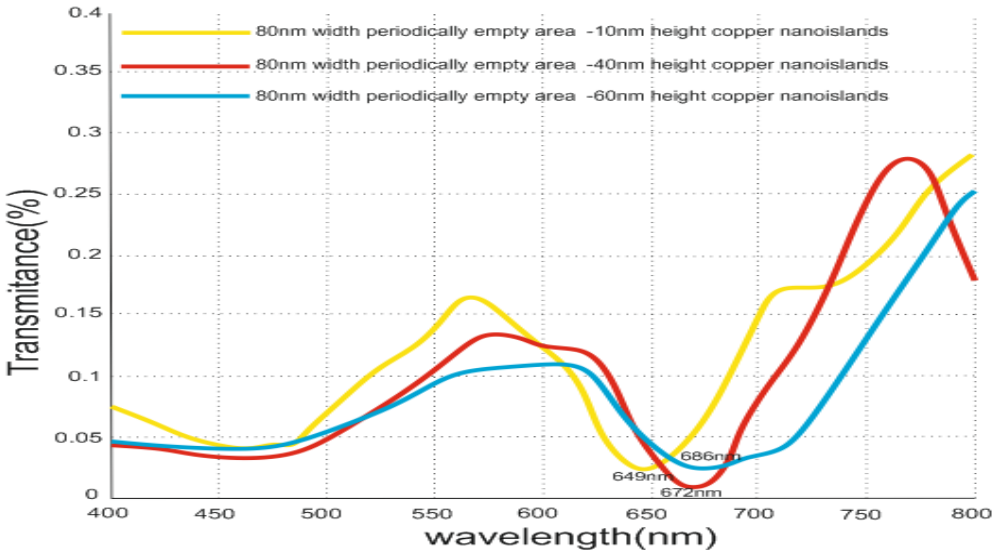

Figure 5.15 : Simulation for 80 nm width periodically empty area with 10,40,60 nm height copper nanoislands

Based on Lumerical simulations, we find that copper nano islands of different heights and densities cause shift in plasmon resonance and the resonance disappears after a certain thickness and density, thus we theoretically prove that plasmonic properties of the surfaces can be electrochemically controlled(Figure 5.12).

In summary, we perform SPR experiments on the samples produced thus demonstrated that different grating structures would show different plasmonic

properties; compatibility of the samples produced with the simulation; and it is consistent with the values in the literature in terms of sensitivity. With experiments performed on the other part of DVD, we observe that important change in surface resonance can be made with depth and period of grating, and the rate of duty cycle only shifts the resonance position. We identify redox current of copper ions using cyclic voltammogram and investigate the voltage value to be used in electrochemical experiments. We then witness that the copper deposited on the surface as nano islands when used SEM, and the density increased with the increased time of voltage application. Finally, we use Lumerical simulation to see how different height and density values of copper nano islands altered the plasmonic properties of surfaces, and we theoretically prove that plasmonic properties of surfaces can be controlled electrochemically.

CHAPTER 6

Electrochemically Switchable Plasmonic Surfaces

As a result of simulations and experiments performed so far, we observe that plasmonic properties of the surfaces can be controlled by electrochemistry. We create controllable plasmonic structures by combining electrochemistry and SPR in this chapter.

6.1 Shallow Grating Experiments

We start our electrochemical SPR experiments with Shallow grating based plasmonic surfaces. Based on the simulations, we expect that the resonance point will be shifted by deposition and stripping; plasmonic properties will disappear after a certain thickness of coating; and plasmonic properties of the surfaces can be reversibly controlled for multiple times if reduction and oxidation reactions are properly controlled. Usage of Keithley power supply in experiments allows precise adjustment of electrical signals. Furthermore, we determine that contact resistance is low in measurements with multimeter thus voltage drops at contact points can be disregarded. Since we know that fluid leakage from the channel would dramatically influence the experiment results, a two-sided band is wrapped around the electrochemical channel for twice. As described in previous chapters, after filling the channel with liquid, it is important to position the small glass in parallel to the ground to prevent bending of upper channel because a skew of 1-2 degrees would result in expected outcomes.

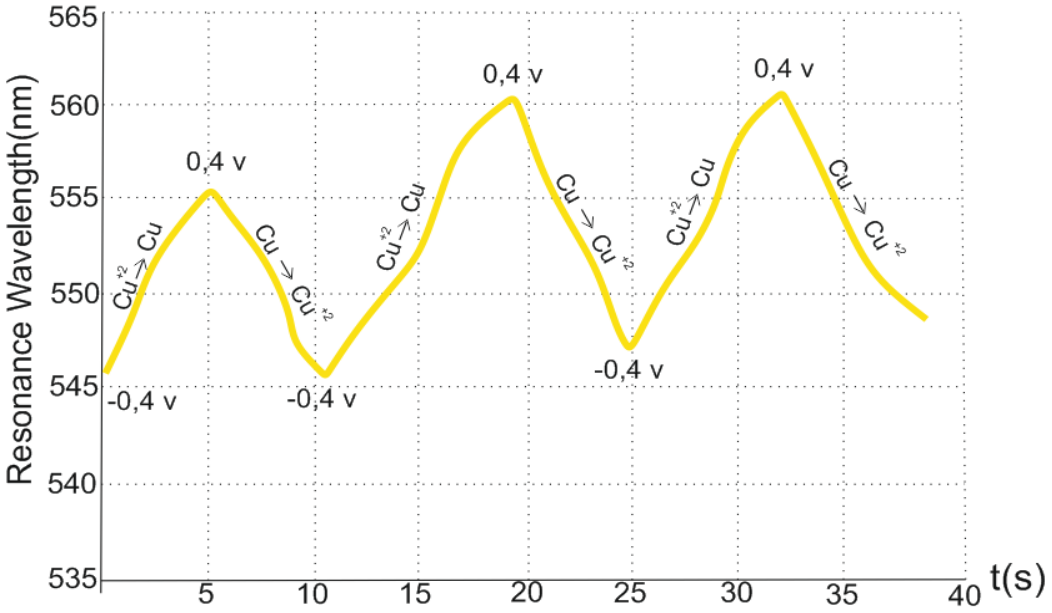

Figure 6.1: ±0,4 V applied voltage; silver as plasmon supporting metallic layer and 0,01 M CuSO4 solution as dielectric media

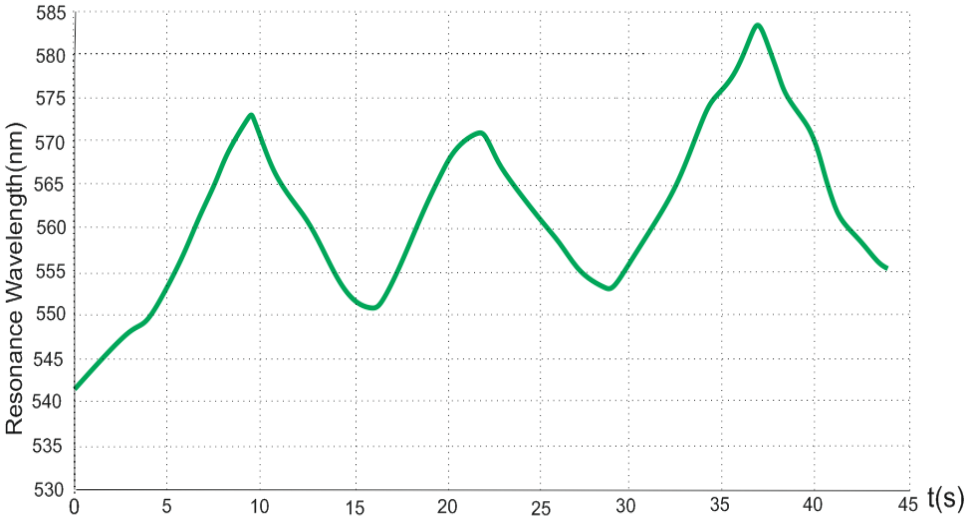

Figure 6.2 : ±0,4 V applied voltage; silver as plasmon supporting metallic layer and 0, 05 M CuSO4 solution as dielectric media

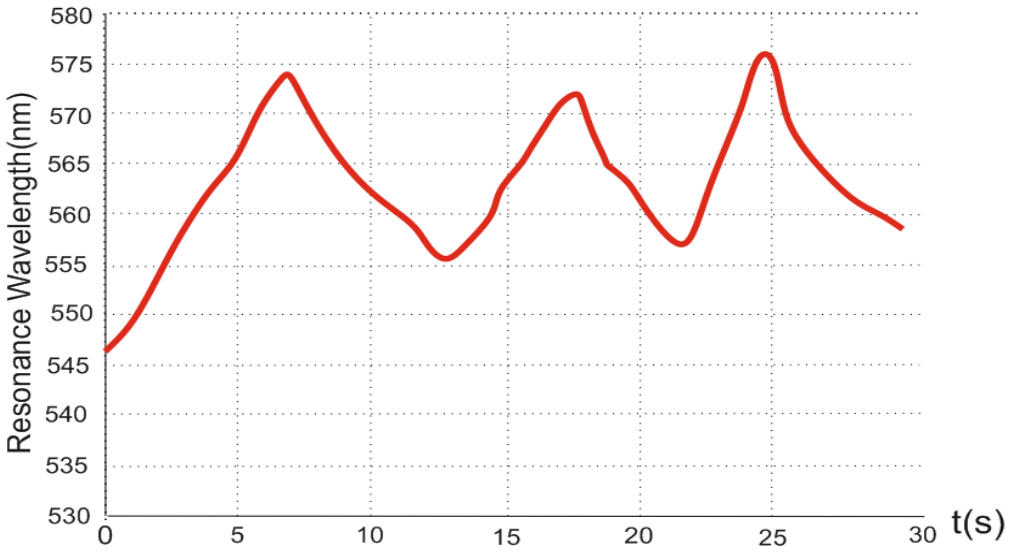

Figure 6.3: ±0,4 V applied voltage; silver as plasmon supporting metallic layer and 0, 1 M CuSO4 solution as dielectric media

In Shallow grating based experiments, we use copper sulfate solutions with different concentrations and the silver as a plasmon supporting layer. Although the main purpose here is to show that plasmonic structures can be controlled electrochemically, we also investigate the effects of different concentrations on plasmonic properties. We determine based on the results of cyclic voltammetry that the voltage to apply should be ±0,4 volt. In this context, we precisely apply the voltages respectively with Keithley power supply. We observe that current indicator of power supply elevates to 1.5 ma at higher concentrations then lower to 100 ua in time depending on the decrease in deposition and stripping. In previous chapter, we prove that the reaction is deposition of copper on the surface and removal from the surface. In this frame, we can argue that the reactions occurred are totally under control. The experiments demonstrate that plasmonic surfaces can be reversibly controlled electrochemically for multiple times. In addition, we find that the resonance point moves further in solutions with high concentration than it do in solutions with low concentration but remain within a certain limit; and it is because, as we mention before, grating structure is impaired by copper deposition as nano islands.

6.2 Deep Grating Experiments

Based on Shallow grating experiments, we expect to observe band pass filter response from Deep grating based plasmonic surfaces. Like the others , we carry out the experiments for different metallic layer and molarity soutions.

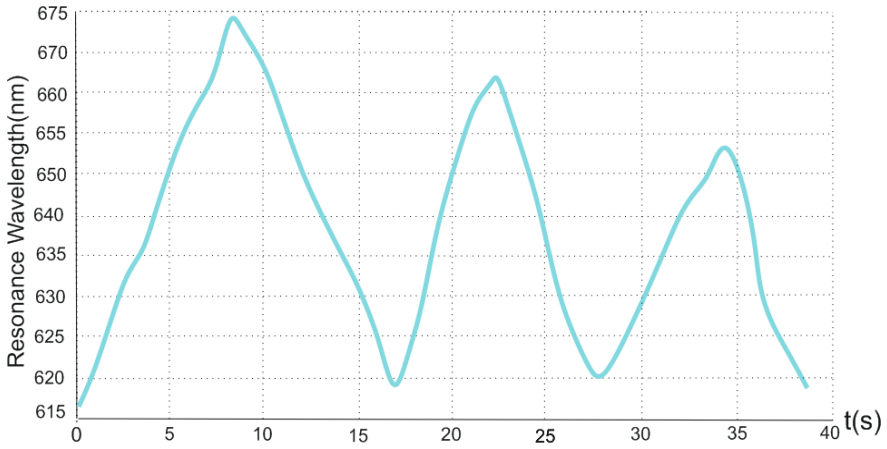

Figure 6.4: ±0,4 V applied voltage; silver as plasmon supporting metallic layer and 0, 02 M CuSO4 solution as dielectric media

We demonstrate the same situtaion that the plasmonic properties of surfaces can be controlled by electrochemistry for Deep grating based plasmonic surfaces Automatically , we produce dynamic band pass filter with 60 nm travel range. (Figure 6.4). We notice that travel range has a limit due to corruption of grating structure, the more copper deposition, the faster corruption in grating structure .

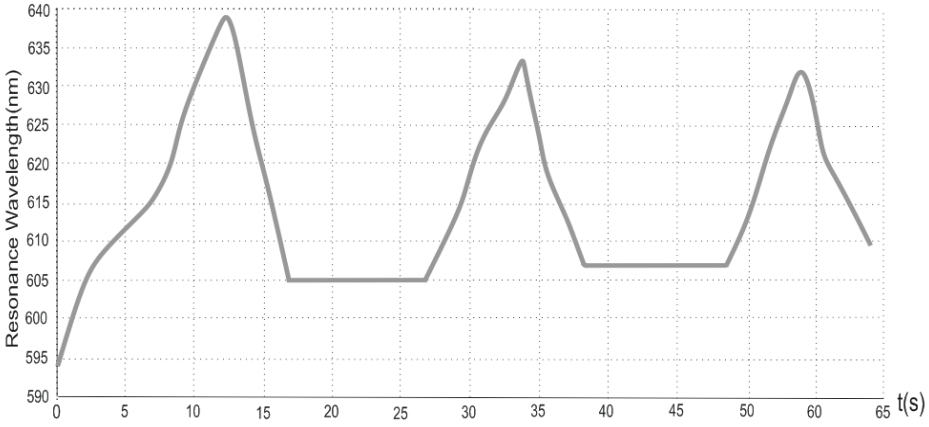

Figure 6.5: ±0,4 V applied voltage; silver as plasmon supporting metallic layer and 0, 05 M CuSO4 solution as dielectric media

We observe whether any undesired reactions occur by disconnecting the link between the electrodes at certain intervals in this experiment. According to the experiment results, no undesired reactions occurr thus it is demonstrated that entire reaction is under control. We determine that resonance do not return to the start point in experiments in which Deep and Shallow grating had silver surface but shows a slow shift. Both to find out the cause of that and to investigate the effects of different voltages and metals, we carry on experiments by changing the voltage into 2 volts and using gold as plasmon supporting metallic layer.

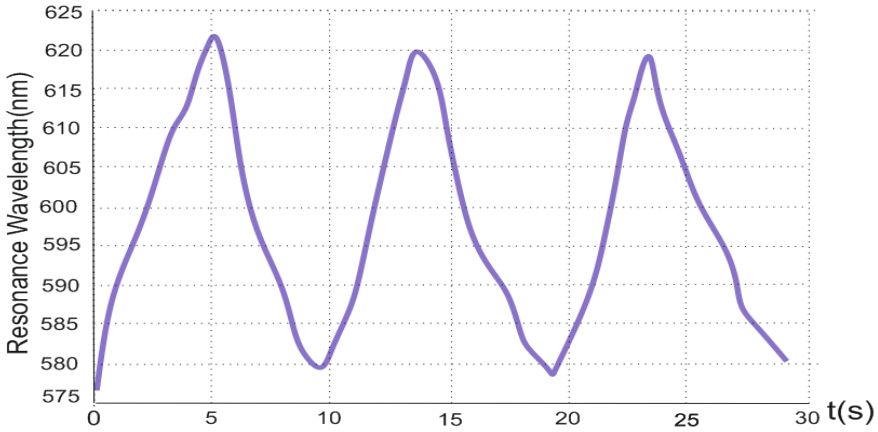

Figure 6.6. ±2V applied voltage; gold as plasmon supporting metallic layer and 0,05 M CuSO4 solution as dielectric media

According to the results of the experiments, the higher voltage applied and gold metallic layer provide improvement in terms of repeatability. One conclusion to derive is that gold is a material that is more preferable in electrochemical applications than silver; and the second conclusion is that there is a problem with silver surfaces. We estimate that silver is stripped from the surface after electrochemical reactions and unable to remove copper fully from the surface. As we mention, germanium provides improvement in terms of adhesive property of silver, stripping problem is still going on, maybe better adhesive layer can solve this problem. Proper adherence of silver to the surface and increased voltage will allow copper to fully remove from the surface. For the time being, the silver is not the metal of choice because of this property of it. We indicate our predictions but since it is not possible to state that directly based on the results of the experiment, we investigate what is going on on the surface by taking images with SEM.

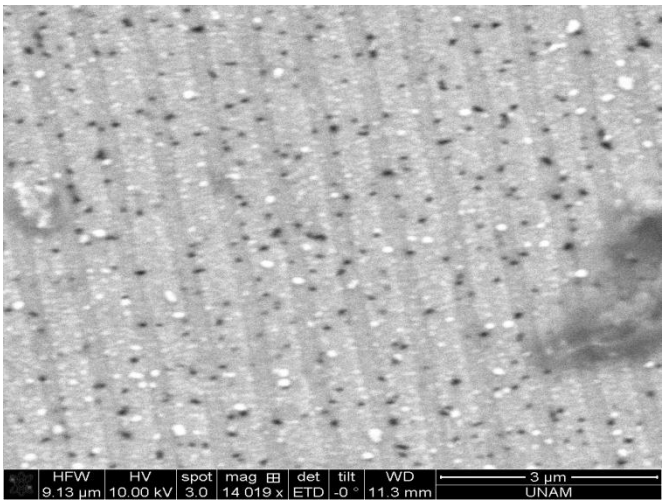

Figure 6.7: Sem image of silver coated grating structure after switched several times

As we expect , silver strips and copper nanoislands locate on surface which we do not expect after oxidation process(Figure 6.7)

In summary, we initially perform electrochemical experiments in different concentrations for Shallow grating structure, and reversibly control plasmonic properties of the surfaces for multiple times. We determine as a result of the experiments that resonance point moves in a larger range when concentration is increased but it has a limit. The resonance disappears after a certain deposition, and it is because copper nano islands deposited on the surface impair the grating structure. What proved theoretically for Shallow grating is also proved practically. As expected, we demonstrate that resonance can be reversibly controlled for multiple times for also Deep grating by repeating the experiments. However, starting point of resonance changes in the experiments in which silver is used as a metallic layer. Then, whether the problem results from copper sulfate or the voltage applied and use of silver is examined by increasing the voltage in gold experiments. As a result, we establish that the problem is caused by the silver but in order to fully understand what it is, we take images of the surface by SEM then observe, as estimated, that the silver is removed from the surface and the copper nano islands remains on the surface after oxidation process. As a solution, we recommend a better adhesive layer and to apply higher voltage. Finally, we achieve to produce the plasmonic based dynamic filters using these two grating structures.

CHAPTER 7

COLORIMETRIC SENSING

7.1. SPR Colorimetric Imaging

Although colorimetry is used to detect alteration as spectrometry, it becomes more important in sensing applications as it decreases dependency on spectrum and is relatively easy to use with simple equipment. The basic logic is based on that alterations are directly detected by change in the color not by analyzing the spectrum. With experiments on refractive index, we demonstrate that resonance point shifts and the color of reflected light is turned after investigating plasmonic properties of Deep grating structures. It is possible to interpret the interactions by detecting changes in the wavelength or angle spectrum in conventional SPR applications. However, based on the studies we perform so far, we can argue that the interactions can be identified only by detecting the change in the color without the need of analyzing the spectrum owing to the Deep grating structure we have developed. Furthermore, we consider that this structure can be used not only for colorimetric sensing but also for displaying nanolayers on the surface. Based on the previous experiments, we determine that golden surfaces are more stable than silver surfaces; we therefore decide to perform colorimetric experiments on the golden surfaces. We create 50 micron width and 150 micron heigh rectangular structures on Deep grating based golden surfaces by optical litography and etching .

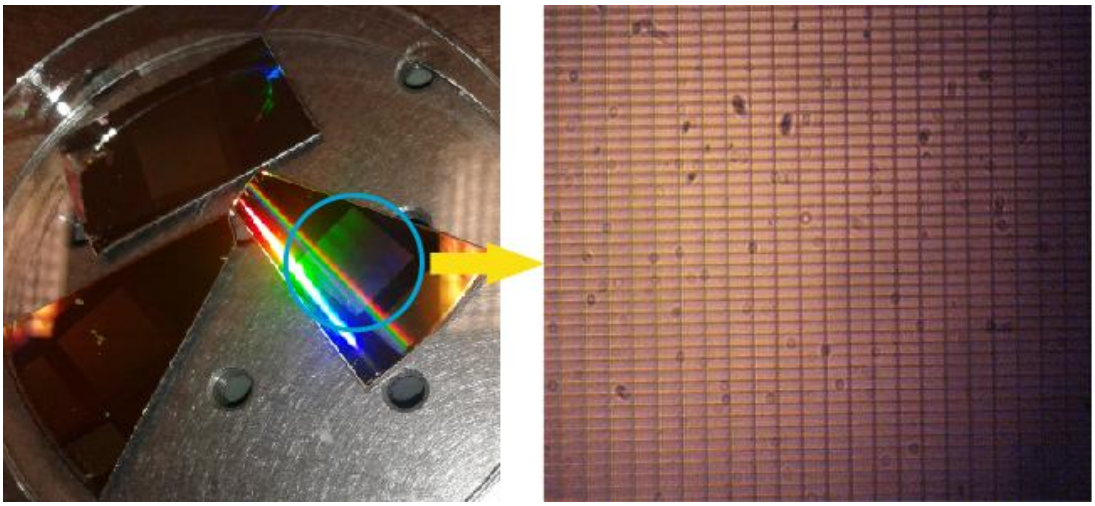

Figure 7.1 . Rectangular structures on Deep grating based golden surface

As seen in the figure 7.1, the golden surface appears in dark red not in yellow and the rectangular structures appear in black. We should indicate that the spots on the image are caused by the dirt on the camera. We perform experiments on gold coated Deep grating based plasmonic surfaces with 0,02 M copper sulfate solution and ±2V applied voltage .

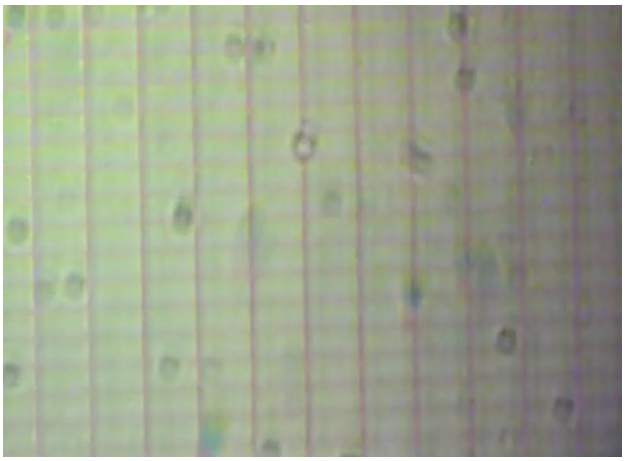

Figure 7.2: Surface image of Deep grating based golden surface with 0,02M CuSO4

As seen in Figure 7.2, golden surface appears in green and the photoresist structures appear in red. The reason of significant difference between the colors with Figure 7.1 and the colors in this figure is that refractive index of copper sulfate solution differs from the refractive index of air. As we set forth above, we perform colorimetric imaging with Deep grating structures. Thus, we prove that it is possible

to display nanolayers on the surface with a simple camera; and that highly detailed images can be achieved by precise cameras.

7.2 SPR Colorimetric Sensing

We then reduce copper on the surface by electrochemically to alter refractive index across the surface, and display copper deposition on the surface with combination of SPR and colorimetry.

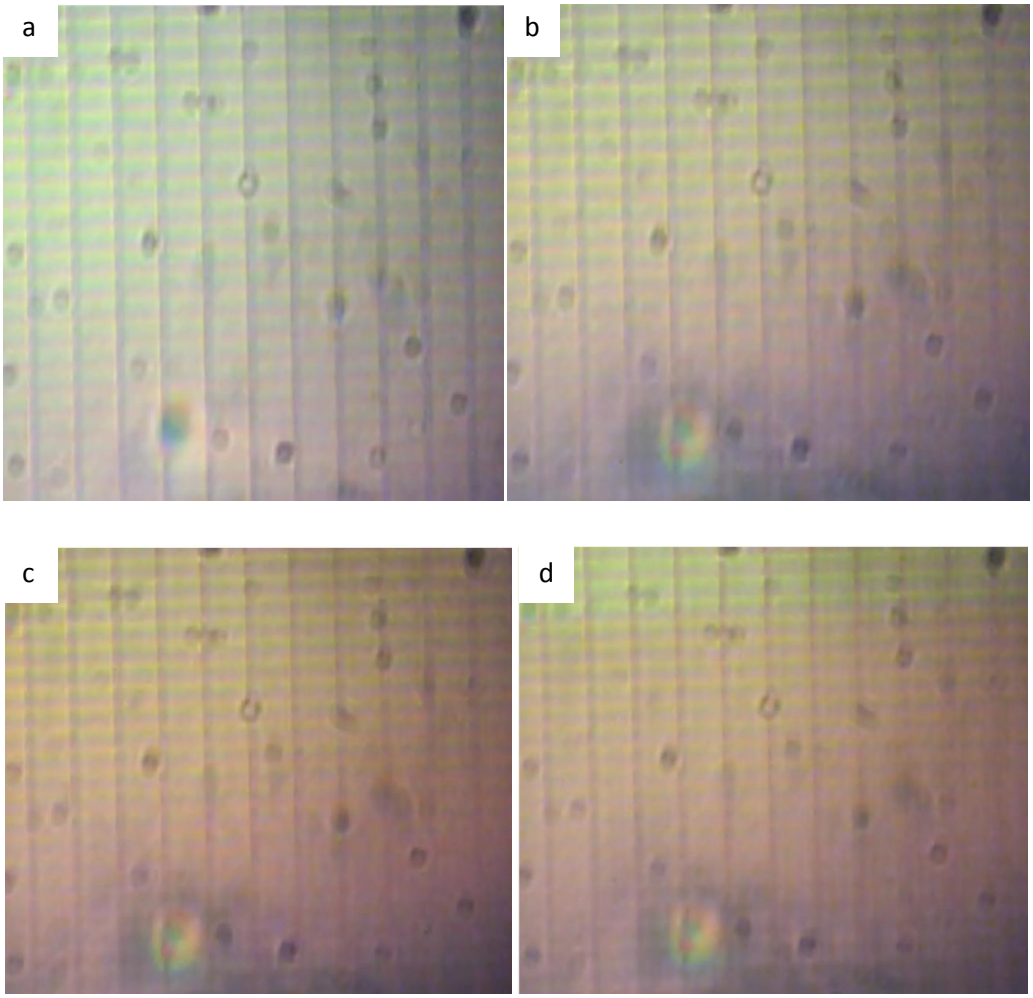

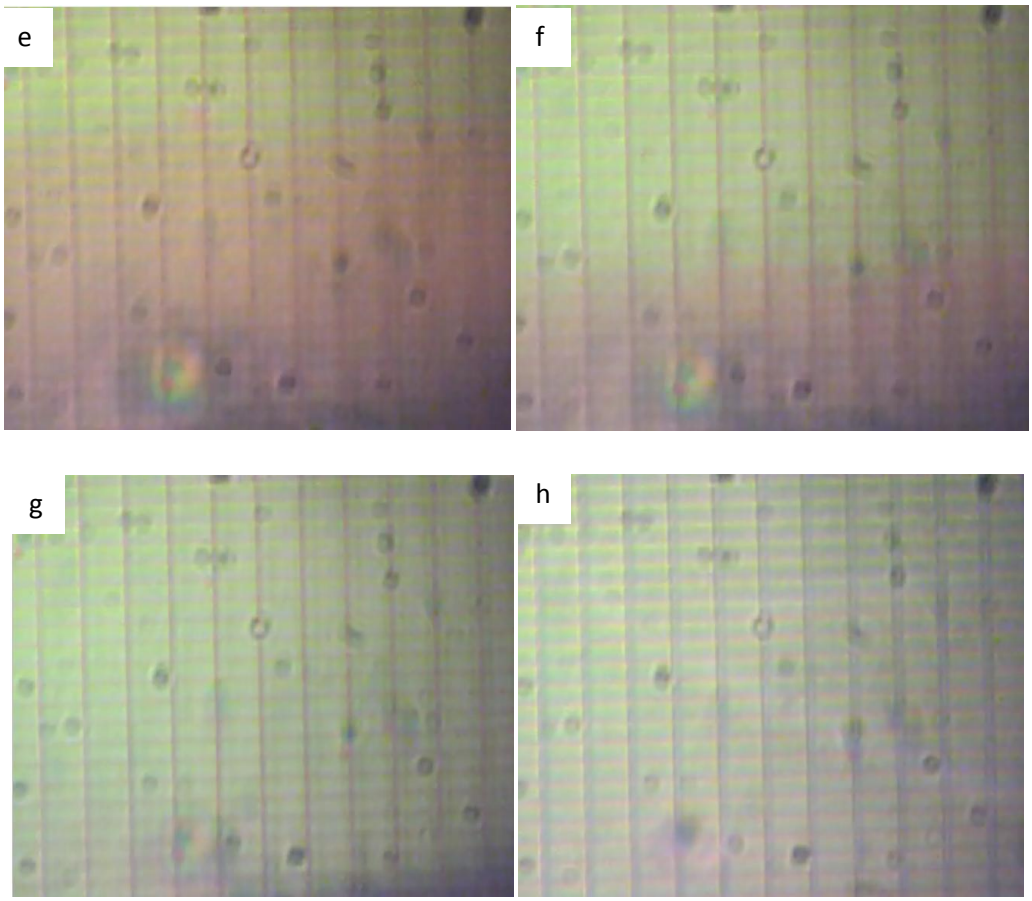

Figure 7.3 : Images of surfaces according to applied voltage

The experiments shows that color of the surface is completely changed when copper is reduced on the surface, and the surface gains its original color in the opposite situation. Reduction of copper here represents the biomolecular interaction and demonstrates that colorimetric measurements can be performed by SPR for biosensor applications.

In summary, by videotaping the structures produced on the surface , we prove that monolayers on the surface can be displayed. We should underline that dirt on the camera lens deteriorated the quality of images. We study and detect the copper reduction on the surface and the color change with electrochemical experiment. It is possible to detect the location of the resonance point by analyzing the colors; in this way we can also analyze it in spectrum. The critical issue here is that the images are taped by a simple camera. Thus, SPR-based colorimetric biosensor applications can be performed by smart phones.

CHAPTER 8

Conclusion and Future work

In this study, we investigate that plasmonic properties of a surface can be electrochemically altered, and performed studies on areas of application. Grating structures are easy to find in the market such as DVDs, and we use AFM to derive surface topography of such structures. The grating depths are grouped into two, Deep and Shallow, depending on the grating depth of DVD grating structures. Then we define plasmonic properties of these grating structures with numerical simulations for different metallic materials and dielectric media. In addition, we determine that reduced copper nanolayers on surface altered plasmonic properties of the surface, thus the surfaces can be electrochemically controlled. We then deposite metal on the surface through thermal evaporator to create simulated structures. We investigate the redox reaction of copper by cyclic voltammetry, and observe that the copper is reduced to surface as nano islands not as nanolayer by SEM. The effects of nano islands on plasmonic properties are investigated by Lumerical software, an advanced simulation program; we theoretically prove that plasmon resonance changed for different thicknesses and densities of copper nano islands. We then practically performe what we prove theoretically by experiments and produced the plasmonic surfaces that can be electrochemically switched. Finally, we perform plasmonic imaging with these surfaces.

However, we address to what needed to be developed during studies; firstly, we emphasize that better adhesive layer needs to be investigated for silver otherwise it would be inappropriate to use in applications. Besides, future works involve repeating experiments for different solutions of copper sulfate. As we describe in previous chapters, we only demonstrate that the structures can be controlled by constant voltage and system with 2 electodes but cyclic voltammogram is required

for more precise control; in this context we produce potentiostat circuit with 3 electrodes.

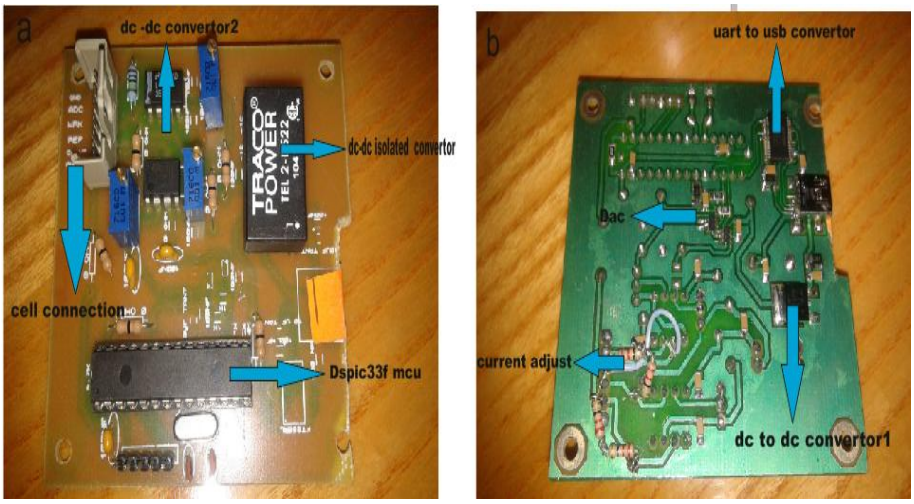

Figure 8.1 ,(a) top view ,(b) bottom view of potantiostat circuit

We use dspic33f microcontroller(MCU). MCU has strong analog to digital convertor unit, so it lets us to measure redox current precisely. Microcontrollers are working in the range of 1,8-5 v but negative voltages must be applied to scan both reduction and oxidation area so dc-dc isolated converter is used . We use 12 bit digital to analog convertor (DAC) called as mcp4725 from microchip to generate applied voltage to electrochemical cell . Dc-dc convertor2 changes the dac outputs to scan negative and positive range. Microcontroller sends current data to computer via usb by uart to usb convertor since no usb unit on dspic33f series microcontollers. We supplied 5v via usb but MCUs are working with 3,3 volt thus we use dc to dc convertor1 to convert voltages. We let user to adjust current range by changing resistor in current-voltage convertor. Through this precise system produced, reduction and oxidation reactions can be controlled more precisely, and we will examine whether formation of nano islands on the surface would be more uniform. We have demonstrated that Deep grating structure can be used in colorimetric imaging; however we know that the main potential is the colorimetric sensing in biosensor applications using this structure. Therefore, we will conduct colorimetric sensing experiments by a simple attachment to smart phones without using expensive equipment. Thus, we believe that we will give a different perspective to SPR based measurements.

Bibliography

[1] *C.Nylander, B.Liedberg, T.Lind," Gas detection by means of surface plasmon resonance", Sensors and Actuators 3, pp79-88, 1982.*

[2] *B. Rothenhausler and W. Knoll, "Surface-plasmon microscopy", Nature, vol. 332, pp. 615, 1988.*

[3] *M. Park, J. Jose, J.Pyun "SPR biosensor by using E. coli outer membrane layer with autodisplayed Z-domains", Sensors and Actuators B: Chemical, Vol. 154, pp. 82-88, 2011*

[4] *H. S. Jang,et al. , "Optical fiber SPR biosensor with sandwich assay for the detection of prostate specific antigen", Optics Communications, Vol. 282, pp.2827-2830, 2009*

[5] *Katrina Campbell, et al., "Comparison of ELISA and SPR biosensor technology for the detection of paralytic shellfish poisoning toxins", Journal of Chromatography B, Vol.877, pp 4079-4089, 2009*

[6] *B.Jeon, M. Kim, J.Pyun ,"Application of parylene film as a linker layer of SPR biosensor", Procedia Chemistry, Vol. 1, pp. 1035-1038, 2009*

[7] *J.W. Chung, S.D. Kim, R. Bernhardt and J.C. Pyun , "Application of SPR biosensor for medical diagnostics of human hepatitis B virus (hHBV)" Sensors and Actuators B: Chemical, Vol.111–112, pp. 416-422, 2005*

[8] *Q. Luan,et al., "Au-NPs enhanced SPR biosensor based on hairpin DNA without the effect of nonspecific adsorption", Biosensors and Bioelectronics, Vol. 26, pp. 2473-2477,2011*

[9] *V. Nanduri,et al., "SPR biosensor for the detection of L. monocytogenes using phage-displayed antibody", Biosensors and Bioelectronics, Vol. 23, pp. 248-252, 2007*

[10] *B.Yakes, et al., "Surface plasmon resonance biosensor for detection of feline calicivirus, a surrogate for norovirus", International Journal of Food Microbiology , Vol. 162, pp. 152-158, 2013*

[11] *J. Chen, et al., "Label-free electrochemical biosensor using home-made 10-methyl-3-nitro-acridone as indicator for picomolar detection of nuclear factor kappa B", Biosensors and Bioelectronics, Vol. 53, pp. 12-17, 2014*

[12] *M. Jarczewska, et al., "Electrochemical uranyl cation biosensor with DNA oligonucleotides as receptor layer", Bioelectrochemistry, Vol. 96, pp. 1-6, 2014*

[13] *S. N.Topkaya, B. Kosova , M.Ozsoz , "Detection of Janus Kinase 2 gene single point mutation in real samples with electrochemical DNA biosensor", Clinica Chimica Acta, Vol. 429, pp.134-139, 2014*

[14] *H. Xu, et al., "Electrochemical DNA nano-biosensor for the detection of genotoxins in water samples", Chinese Chemical Letters, Vol. 25, pp. 29-34, 2014*

[15] *F. Li, et al., "Carbon nanotube-based label-free electrochemical biosensor for sensitive detection of miRNA-24", Biosensors and Bioelectronics, Vol. 54, pp. 158-164 ,2014*

[16] *Z. Yi ,et al. ,"A novel electrochemical biosensor for sensitive detection of telomerase activity based on structure-switching DNA", Biosensors and Bioelectronics, Vol.53, pp. 310-315, 2014*

[17] *Y. Tang ,et al., "A novel electrochemical biosensor for monitoring protein nitration damage affected by $NaNO_2$/hemin/H_2O_2", Biosensors and Bioelectronics, Vol. 54, pp. 628-633, 2014*

[18] *X. Han, et al., "An electrochemical DNA biosensor based on gold nanorods decorated graphene oxide sheets for sensing platform", Analytical Biochemistry, Vol. 443, pp. 117-123, 2013*

[19] *Y. Guo, J. Chen , G. Chen ," A label-free electrochemical biosensor for detection of HIV related gene based on interaction between DNA and protein", Sensors and Actuators B: Chemical, Vol. 184, pp. 113-117, 2013*

[20] *A. Li, Y. Ma, F. Yang, X. Yang , "Interaction between α-actinin and negatively charged lipids membrane investigated by surface plasmon resonance and electrochemical methods" , Applied Surface Science, Vol.253, pp. 6103-6108, 2007*

[21] *K. Toda,et al., "Electrochemical enzyme immunoassay using immobilized antibody on gold film with monitoring of surface plasmon resonance signal " Analytica Chimica Acta, Vol. 463, pp. 219-227, 2002*

[22] *Y. M. Panta,et al., "Ultrasensitive detection of mercury (II) ions using electrochemical surface plasmon resonance with magnetohydrodynamic convection ", Journal of Colloid and Interface Science, Vol.333 , pp.485-490, 2009*

[23] *X. Huang, et al. ,"Flow-through Electrochemical Surface Plasmon Resonance: Detection of intermediate reaction products ", Journal of Electroanalytical Chemistry, Vol.649, pp. 37-41, 2010*

[24] *M.Vasjari, et al., " SPR investigation of mercury reduction and oxidation on thin gold electrodes", Journal of Electroanalytical Chemistry, Vol. 605, pp.73-76, 2007*

[25] *A. Tsuboi , K.Nakamura and N. Kobayashi ," A Localized Surface Plasmon Resonance-Based Multicolor Electrochromic Device with Electrochemically Size-Controlled Silver Nanoparticles", Advanced Materials, Vol. 25, 2013*

[26] *X. Shan , et al. ," Imaging Local Electrochemical Current via Surface Plasmon Resonance " ,Vol 1363, 2010*

[27] *E. Kretschmann and H. Raether, Dynamic all-optical tuning of transverse resonant cavity modes in photonic bandgap fibers, Z Naturforschung, vol. 23a, p. 2135, 1968*

[28] *A. Otto, Towards multimaterial multifunctional fibres that see, hear, sense and communicate, Zeitschrift fur Physik, vol. 216, pp. 398–410, 1968*

[29] *J. M. Hollander , W. L. Jolly ," X-ray photoelectron spectroscopy", Acc. Chem. Res. , 1970*

[30] *Y. Kaya , et al., " Sensitivity comparasion of localized plasmon resonance structures and prism coupler " , Sensors and Actuators B: Chemical , Vol. 191, pp. 516-521 , 2014*